

1     Root hair-endophyte stacking (RHESt) in an ancient Afro-Indian crop creates an  
2                                   unusual physico-chemical barrier to trap pathogen(s)

3  
4     W. K. Mousa<sup>1</sup>, C. Shearer<sup>1</sup>, Victor Limay-Rios<sup>2</sup>, C. Ettinger<sup>3</sup>, J. A. Eisen<sup>3</sup>, and M.N. Raizada<sup>1</sup>

5     <sup>1</sup>Department of Plant Agriculture, University of Guelph, Guelph, ON Canada N1G 2W1

6     <sup>2</sup>Department of Plant Agriculture, University of Guelph, Ridgetown Campus, Ridgetown, ON,  
7     Canada, N0P 2C0

8     <sup>3</sup>University of California Davis Genome Center, Davis, California, USA 95616

9  
10    \*Author for correspondence:

11    Manish N. Raizada

12    Email: [raizada@uoguelph.ca](mailto:raizada@uoguelph.ca); Phone 1-519-824-4120 x53396; FAX 1-519-763-8933

13

14

15

16

17

18

19 **The ancient African crop, finger millet, has broad resistance to pathogens including the**  
20 **toxigenic fungus *Fusarium graminearum*. Here we report the discovery of a novel plant**  
21 **defence mechanism, resulting from an unusual symbiosis between finger millet and a root-**  
22 **inhabiting bacterial endophyte, M6 (*Enterobacter* sp.). Seed-coated M6 swarms towards**  
23 ***Fusarium* attempting to penetrate root epidermis, induces growth of root hairs which then**  
24 **bend parallel to the root axis, then forms biofilm-mediated microcolonies, resulting in a**  
25 **remarkable, multi-layer root hair-endophyte stack (RHESt). RHESt results in a physical**  
26 **barrier that prevents entry and/or traps *F. graminearum* which is then killed. Thus M6**  
27 **creates its own specialized killing microhabitat. M6 killing requires c-di-GMP-dependent**  
28 **signalling, diverse fungicides and xenobiotic resistance. Further molecular evidence**  
29 **suggests long-term host-endophyte-pathogen co-evolution. The end-result of this**  
30 **remarkable symbiosis is reduced DON mycotoxin, potentially benefiting millions of**  
31 **subsistence farmers and livestock. RHESt demonstrates the value of exploring ancient,**  
32 **orphan crop microbiomes.**

33

## 34 **Introduction**

35 Finger millet (*Eleusine coracana*) is a cereal crop widely grown by subsistence farmers in  
36 Africa and South Asia<sup>1,2</sup>. Finger millet was domesticated in Western Uganda and Ethiopia  
37 around 5000 BC then reached India by 3000 BC<sup>3</sup>. With few exceptions, subsistence farmers  
38 report that finger millet is widely resistant to pathogens including *Fusarium* species<sup>4,5</sup>. One  
39 species of *Fusarium*, *F. graminearum*, causes devastating diseases in crops related to finger  
40 millet including maize, wheat and barley, associated with accumulation of the mycotoxin  
41 deoxynivalenol (DON) which affects humans and livestock<sup>6,7</sup>. However, despite its prevalence  
42 as a disease-causing agent across cereals, *F. graminearum* is not considered to be an important  
43 pathogen of finger millet, suggesting this crop has tolerance to this *Fusarium* species<sup>4,8</sup>.

44

45 The resistance of finger millet grain to fungal disease has been attributed to high  
46 concentrations of polyphenols<sup>9,10</sup>. However, emerging literature suggests that microbes that  
47 inhabit plants without themselves causing disease, defined as endophytes, may contribute to host  
48 resistance against fungal pathogens<sup>11,12</sup>. Endophytes have been shown to suppress fungal  
49 diseases through induction of host resistance genes<sup>13</sup>, competition<sup>14</sup>, and/or production of anti-  
50 pathogenic natural compounds<sup>15,16</sup>.

51

52 *Fusarium* are ancient fungal species, dating to at least 8.8 million years ago, and their  
53 diversification appears to have co-occurred with that of the C4 grasses (which includes finger  
54 millet), certainly pre-dating finger millet domestication in Africa<sup>17</sup>. Multiple studies have  
55 reported the presence of *Fusarium* in finger millet in Africa and India<sup>18-23</sup>. A diversity of *F.*

56 *verticillioides* (synonym *F. moniliforme*) has been observed in finger millet in Africa and it has  
57 been suggested that the species evolved there<sup>18</sup>. These observations suggest the possibility of co-  
58 evolution within finger millet between *Fusarium* and millet endophytes. We previously isolated,  
59 for the first time, fungal endophytes from finger millet and showed that their natural products  
60 have anti-*Fusarium* activity<sup>4</sup>. We could not find reports of bacterial endophytes isolated from  
61 finger millet.

62

63 The objectives of this study were to isolate bacterial endophytes from finger millet, assay  
64 for anti-*Fusarium* activity and characterize the underlying cellular, molecular and biochemical  
65 mechanisms. We report an unusual symbiosis between the host and a root-inhabiting bacterial  
66 endophyte.

67

## 68 **Results**

### 69 **Isolation, identification and antifungal activity of endophytes**

70 A total of seven bacterial endophytes were isolated from surface-sterilized tissues of finger  
71 millet, strains M1 to M7 (Fig. 1a-c and Supplementary Table 1). BLAST searching of the 16S  
72 rDNA sequences against Genbank suggested that strains M1 and M6 resemble *Enterobacter* sp.  
73 while M2 and M4 resemble *Pantoea* sp., and M3, M5, and M7 resemble *Burkholderia* sp..  
74 GenBank accession numbers for strains M1, M2, M3, M4, M5, M6 and M7 are KU307449,  
75 KU307450, KU307451, KU307452, KU307453, KU307454, and KU307455, respectively. The  
76 16S rDNA sequences for finger millet bacterial endophytes were used to generate a phylogenetic

77 tree (Supplementary Fig.1) using Phylogeny.fr software<sup>24,25</sup>. Interestingly, five of the seven strains  
78 showed anti-fungal activity against *F. graminearum in vitro* (Fig. 1c-d). Strain M6 from millet  
79 roots showing the most potent activity and hence was selected for further study including whole  
80 genome sequencing, which resulted in a final taxonomic classification (*Enterobacter* sp., strain  
81 UCD-UG\_FMILLET)<sup>26</sup>. M6 was observed to inhibit the growth of 5 out of 20 additional crop-  
82 associated fungi, including pathogens, suggesting it has a wider target spectrum (Supplementary  
83 Table 2). As viewed by electron microscopy, M6 showed an elongated rod shape with a wrinkled  
84 surface (Fig. 1e). Following seed coating, GFP-tagged M6 localized to finger millet roots  
85 intercellularly and intracellularly (Fig. 1f,g). In addition, colonization of finger millet with M6  
86 did not result in pathogenic symptoms (Supplementary Fig. 2). Combined, these results confirm  
87 that M6 is an endophyte of finger millet.

88

89 To determine whether strain M6 has anti-*Fusarium* activity *in planta*, related *Fusarium*-  
90 susceptible cereals (maize and wheat) were used as model systems (Fig. 1 h-r), since finger  
91 millet itself is not reported to be susceptible to *F. graminearum*. Seed-coated GFP-tagged M6  
92 was shown to colonize the internal tissues of maize (Fig. 1h) and wheat (Fig. 1n) suggesting it  
93 can also behave as an endophyte in these crop relatives. Treatments (combined seed coating and  
94 foliar spray) with M6 caused statistically significant ( $P \leq 0.05$ ) reductions in *F. graminearum*  
95 disease symptoms in maize (Gibberella Ear Rot, Fig. 1i-l) and wheat (Fusarium Head Blight, Fig.  
96 1o-q) ranging from 70 to 90% and 20-30%, respectively in two greenhouse trials, compared to  
97 plants treated with *Fusarium* only (yield data in Supplementary Fig. 3a-b; Supplementary Table  
98 3). Foliar spraying alone with M6 resulted in more disease reduction compared to seed coating  
99 alone, though this effect was not statistically significant, at  $P \leq 0.05$  (Supplementary Fig. 3c).

100 Following extended storage to mimic those of African subsistence farmers (ambient temperature  
101 and moisture), treatment with M6 resulted in dramatic reductions in DON accumulation, with  
102 DON levels declining from ~3.4 ppm to 0.1 ppm in maize, and from 5.5 ppm to 0.2 ppm in  
103 wheat, equivalent to 97% and 60% reductions, respectively, compared to plants treated with  
104 *Fusarium* only, at  $P \leq 0.05$  (Fig. 1m,r and Supplementary Table 4).

105

### 106 **Microscopic imaging of M6-*Fusarium* interactions in finger millet roots and *in vitro***

107 Since *F. graminearum* has been reported to infect cereal roots<sup>27</sup>, and since endophyte M6  
108 was originally isolated from the same tissue, finger millet roots were selected to visualize  
109 potential interactions between M6 and *F. graminearum* (Fig. 2). GFP-tagged M6 was coated  
110 onto millet seed. Following germination (Fig. 2a), GFP-M6 showed sporadic, low population  
111 density distribution throughout the seminal roots (Fig. 2b). Following inoculation with *F.*  
112 *graminearum*, which was visualized using calcofluor staining, GFP-M6 accumulated at sites of  
113 attempted entry by *Fusarium*, creating a remarkable, high density layer of microcolonies of M6  
114 along the entire root epidermal surface, the rhizoplane (Fig. 2c,d). External to the M6 rhizoplane  
115 barrier was a thick mat of root hairs (RH) (Fig. 2c,d). RH number and length were much greater  
116 at sites of M6 accumulation compared to the opposite side (Fig. 2c), and M6 was shown *in vitro*  
117 to produce auxin (Supplemental Method 1, Supplementary Fig. 4), a known RH-growth  
118 promoting plant hormone<sup>28</sup>. Interestingly, most RH were bent, parallel to the root axis (Fig. 2d).  
119 The RH mat appeared to obscure M6 cells, and when observed in a low RH density area (Fig.  
120 2e), M6 cells were clearly visible and appeared to attach onto root hairs and engulf *Fusarium*  
121 hyphae (Fig. 2f). Imaging at deeper confocal planes below the surface of the RH mat (Fig. 2g,h)

122 revealed that the mat did not consist only of RH, but rather that M6 cells were intercalated  
123 between bent RH strands forming an unusual, multi-layer root hair-endophyte stack (RHESt).  
124 Within the RHESt, *F. graminearum* hyphae appeared to be trapped (Fig. 2h). By imaging only  
125 the M6-*Fusarium* interaction within the RHESt, M6 microcolonies were observed to be  
126 associated with breakage of the fungal hyphae (Fig. 2i,j). To confirm that the endophyte actively  
127 kills *Fusarium*, Evans blue vitality stain, which stains dead hyphae blue, was used following co-  
128 incubation on a microscope slide. The fungal hyphae in contact with strain M6 stained blue and  
129 appeared broken (Fig. 3a) in contrast to the control (*F. graminearum* exposed to buffer only)  
130 (Fig. 3b). The M6 result was similar to the well known fungicidal activity of the commercial  
131 biocontrol agent, *B. subtilis* (Fig. 3c). Combined, these results suggest that M6 cooperates with  
132 RH cells to create a specialized killing microhabitat (RHESt) that protects millet roots from  
133 invasion by *F. graminearum*.

134

135         Since M6, in the absence of *Fusarium*, was sporadically localized *in planta*, but then  
136 accumulated at sites of *Fusarium* hyphae, it was hypothesized that M6 actively seeks *Fusarium*.  
137 To test this hypothesis, GFP-tagged M6 and *F. graminearum* were spotted adjacent to one  
138 another on a microscope slide coated with agar; as time progressed, M6 was observed to swarm  
139 towards *Fusarium* hyphae (Fig. 3d-i), confirming its ability to seek *Fusarium*. Upon finding the  
140 pathogen, M6 cells were observed to physically attach onto *F. graminearum* hyphae (Fig. 3g-i).  
141 At the endpoint of these interactions, dense microcolonies of M6 were observed to break the  
142 hyphae (Fig. 3j). Transmission electron microscopy showed that M6 possesses multiple  
143 peritrichous flagella (Fig. 3k). Since this interaction was observed *in vitro*, independent of the  
144 host plant, the data show that M6 alone is sufficient to exert its fungicidal activity. To test if the

145 attachments of M6 observed *in vitro* and *in planta* are mediated by biofilm formation, the  
146 proteinaceous biofilm matrix stain, Ruby Film Tracer (red), was used *in vitro*. Red staining,  
147 indicating biofilm formation, was observed associated with M6 in the absence of *Fusarium* (Fig.  
148 3l). In the presence of *F. graminearum*, biofilm was also observed on the hyphal surfaces (Fig.  
149 3m). Combined, these results suggest that M6 cells swarm towards *Fusarium* hyphae attempting  
150 to penetrate the root epidermis, induces root hair growth and bending, resulting in formation of  
151 RHESt within which M6 cells form biofilm-mediated microcolonies which attach, engulf and  
152 kill *Fusarium*.

153

#### 154 **Identification of strain M6 genes required for anti-*Fusarium* activity**

155 Since the fungicidal activity of M6 was observed to occur independently of its host plant,  
156 M6 was subjected to Tn5 mutagenesis and then candidate Tn5 insertions were screened *in vitro*  
157 for loss of fungicidal activity against *F. graminearum*. Out of 4800 Tn5 insertions that were  
158 screened in triplicate, sixteen mutants were isolated that resulted in loss or reduction in the  
159 diameter of inhibition zones of *F. graminearum* growth (Supplementary Fig. 5a). The mutants  
160 that resulted in complete loss of the antifungal activity *in vitro* were validated for loss of anti-  
161 *Fusarium* activity *in planta* in two independent greenhouse trials in maize (Supplementary Fig.  
162 5b,c), demonstrating the relevance of the *in vitro* results. Rescue of the Tn5-flanking sequences  
163 followed by BLAST searching against the whole genome wild type M6<sup>26</sup>, resulted in the  
164 successful identification of 13 candidate genes in 12 predicted operons (Supplementary Table 5  
165 and 6). Based on gene annotations and the published literature, four regulatory and/or anti-  
166 microbial mutants of interest were selected, complemented (Supplementary Fig. 5d) and

167 subjected to detailed characterization. The selected genes encode two LysR family  
168 transcriptional regulators, a diguanylate cyclase, and a colicin V biosynthetic enzyme:

### 169 **LysR transcription regulator in a phenazine operon (*ewpR-5D7::Tn5*)**

170 *Ewp-5D7::Tn5* resulted in complete loss of the antifungal activity *in vitro* (Supplementary  
171 Fig. 5a) and reduction in activity *in planta* (Fig. 4a). The Tn5 insertion was localized to an  
172 operon (*ewp*, Fig. 4b) that included tandem paralogs of *phzF* (*ewpF1* and *ewpF2*) (trans-2,3-  
173 dihydro-3-hydroxyanthranilate isomerase, EC # 5.3.3.17), a homodimer enzyme that forms the  
174 core skeleton of phenazine, a potent anti-fungal compound<sup>29</sup>. The insertion occurred within a  
175 member of the LysR transcriptional regulator family (*ewpR*), which has been previously reported  
176 to induce phenazine biosynthesis<sup>30</sup>. Three lines of evidence suggest the LysR gene is an  
177 upstream regulator of the *ewp* operon. First, the genomic organization showed that LysR was  
178 transcribed in the opposite direction as the operon. Second, the LysR canonical binding site  
179 sequence (TN<sub>11</sub>A) was observed upstream of the *phzF* (*ewaF*) coding sequences<sup>31</sup> (Fig. 4b).  
180 Finally, real time PCR revealed that the expression of *ewpF1* and *ewpF2* were dramatically  
181 down-regulated in the LysR mutant compared to wild type (Fig. 4c). Combined, these results  
182 suggest that EwpR is a regulator of phenazine biosynthesis in strain M6 (Fig. 4d). The crude  
183 methanolic extract from EwpR-5D7::Tn5 lost anti-*Fusarium* activity *in vitro* in contrast to  
184 extracts from wild type M6 or randomly selected Tn5 insertions that otherwise had normal  
185 growth rates (Fig. 4e). Anti-*F. graminearum* bioassay guided assay fractionation using extracts  
186 from M6 showed two active fractions (A, B) (Fig. 4e-g), each containing a compound with a  
187 diagnostic fragmentation pattern of [M+H]<sup>+</sup>=181.0, corresponding to a phenazine nucleus  
188 (C<sub>12</sub>H<sub>8</sub>N<sub>2</sub>, MW = 180.08)<sup>32</sup>, and molecular weights (M+Z= 343.3 and 356.3) indicative of  
189 phenazine derivatives [griseolutein A (C<sub>17</sub>H<sub>14</sub>N<sub>2</sub>O<sub>6</sub>, MW= 342.3) and D-alanyl-griseolutein

190 (C<sub>18</sub>H<sub>17</sub>N<sub>3</sub>O<sub>5</sub>, MW=355.3), respectively]<sup>33-35</sup>. Surprisingly, the *ewp* mutant showed a significant  
191 reduction in motility (Fig. 4h) and swarming (Fig. 4i) compared to the wild type (Fig. 4j),  
192 concomitant with a ~60 % reduction in flagella (Fig. 4k) compared to wild-type (Fig. 3k), loss of  
193 attachment to *Fusarium* hyphae (Fig. 4l) compared to wild-type (inset in Fig. 4l), as well as  
194 reductions in biofilm formation (Fig. 4m,n). Combined, these results suggest that *ewpR* is  
195 required for multiple steps in the anti-fungal pathway of M6 including phenazine biosynthesis.

196

### 197 **LysR transcriptional regulator in a fusaric acid resistance pump operon (*ewfR-7D5::Tn5*)**

198 *EwfR-5D7::Tn5* resulted in a significant loss of the antifungal activity *in vitro*  
199 (Supplementary Fig. 5a). The Tn5 insertion occurred in an operon (*ewf*, Fig. 5a) that included  
200 genes that encode membrane proteins required for biosynthesis of the fusaric acid efflux pump  
201 including a predicted *fusE*-MFP/HIYD membrane fusion protein and *fusE* (*ewfD* and *ewfE*,  
202 respectively) and other membrane proteins (*ewfB*, *ewfH* and *ewfI*)<sup>36,37</sup>. Fusaric acid (5-  
203 butylpyridine-2-carboxylic acid) is a mycotoxin that is produced by *Fusarium* which interferes  
204 with bacterial growth and metabolism and alters plant physiology<sup>38,39</sup>. Bacterial-encoded fusaric  
205 acid efflux pumps promote resistance to fusaric acid<sup>40,41</sup>. Consistent with expectations, *EwfR*-  
206 5D7::Tn5 failed to grow on agar supplemented with fusaric acid compared to the wild type (Fig.  
207 5b,c). The Tn5 insertion specifically occurred within a member of the LysR transcriptional  
208 regulator family (*ewfR*). Similar to *ewpR* above and a previously published fusaric acid  
209 resistance operon<sup>41</sup>, the regulator was transcribed in the opposite direction as the *ewf* operon,  
210 with this genomic organization suggesting that *ewfR* may be an upstream regulator of the operon.  
211 Indeed, the LysR canonical binding site sequence (TN<sub>11</sub>A) was observed upstream of the *ewfB-J*

212 coding sequences<sup>31</sup> (Fig. 5a). Finally, real time PCR revealed that the expression of *ewfD* and  
213 *ewfE* were dramatically downregulated in the LysR mutant compared to wild type (Fig. 5d).  
214 Combined, these results suggest that EwfR is a positive regulator of the *ewf* fusaric acid  
215 resistance operon in strain M6.

216

217 In addition, the *ewf* mutant showed a significant reduction in motility (Fig. 5e) and  
218 swarming (Fig. 5f) compared to the wild type (Fig. 5g), concurrent with a ~30 % reduction in  
219 flagella (Fig. 5h) compared to the wild-type (Fig. 3k). The mutant also showed loss of  
220 attachment to *Fusarium* hyphae (Fig. 5i) compared to wild-type (inset) and reductions in biofilm  
221 formation (Fig. 4j,k). Combined, these results suggest that strain M6 expression of resistance to  
222 fusaric acid is a pre-requisite step that enables subsequent anti-fungal steps.

223

#### 224 **Interaction between the phenazine biosynthetic operon (*ewp*) and the fusaric acid** 225 **resistance operon (*ewf*)**

226 The expression of *ewfR* (LysR regulator of fusaric acid resistance) increased two-fold in  
227 the presence of *Fusarium* mycelium *in vitro* after 1 h of co-incubation, and tripled after 2 h (Fig.  
228 5l). Expression of *ewfR* was also up-regulated by fusaric acid alone (Fig. 5l), demonstrating that  
229 the resistance operon is inducible. Fusaric acid has been shown to suppress phenazine  
230 biosynthesis through suppression of quorum sensing regulatory genes<sup>42</sup>. Interestingly,  
231 expression of the putative LysR regulator of phenazine biosynthesis (*ewpR*, see above) was  
232 downregulated by fusaric acid at log phase (2.5-3 h), but only when fusaric acid resistance was  
233 apparently lost (*ewfR* mutant) (Fig. 5m) compared to wild type (Fig. 5n), suggesting that fusaric

234 acid normally represses phenazine biosynthesis in M6. These results provide evidence for an  
235 epistatic relationship between the two LysR mutants required for the anti-*Fusarium* activity.

236

### 237 **Diguanylate cyclase (*ewgS*-10A8::Tn5)**

238 *EwgS*-10A8::Tn5 resulted in a significant loss of the antifungal activity *in vitro*  
239 (Supplementary Fig. 5a). The Tn5 insertion occurred in a coding sequence encoding diguanylate  
240 cyclase (EC 2.7.7.65) (*ewgS*) that catalyzes conversion of 2-guanosine triphosphate to c-di-GMP,  
241 a secondary messenger that mediates quorum sensing and virulence traits<sup>43</sup> (Fig. 6a). Addition  
242 of exogenous c-di-GMP to the growth medium restored the antifungal activity of the mutant  
243 (Fig. 6b). Real time PCR showed that *ewgS* is not inducible by *Fusarium* (Fig. 6c). Consistent  
244 with its predicted upstream role in regulating virulence traits, the *ewg* mutant showed dramatic  
245 losses in motility (Fig. 6d), swarming (Fig. 6e, compared to wild-type Fig. 6f) and flagella  
246 formation (~40 % reduction, Fig. 6g compared to wild-type, Fig. 3k). Attachment to *Fusarium*  
247 hyphae (Fig. 6h) and biofilm formation (Fig. 6i-j) appeared to have been lost completely.

248

### 249 **Colicin V production protein (*EwvC*-4B9::Tn5)**

250 *EwvC*-4B9::Tn5 showed significant loss of the antifungal activity *in vitro* (Supplementary  
251 Fig. 5a). The Tn5 insertion occurred in a minimally characterized gene required for colicin V  
252 production (*ewvC*) orthologous to *cvpA* in *E.coli*<sup>44</sup>. Colicin V is a secreted peptide antibiotic<sup>45</sup>.  
253 Consistent with the gene annotation, *EwvC*-4B9::Tn5 failed to inhibit the growth of an *E. coli*  
254 strain that is sensitive to colicin V, compared to the wild type (Fig. 7a). Real time PCR showed

255 that the expression of *ewvC* increased 6-fold after co-incubation with *Fusarium* at log phase (Fig.  
256 7b). The mutant showed only limited changes in other virulence traits, including reductions in  
257 motility (Fig. 7c) and swarming (Fig. 7d, compared to wild-type, Fig. 7e), but with only a ~15%  
258 minor reduction in flagella formation (Fig. 7f, compared to wild-type, Fig. 3k), no obvious  
259 change in attachment to *Fusarium* hyphae (Fig. 7g), and only a slight reduction in biofilm  
260 formation (Fig. 7h,i).

261

## 262 **Discussion**

### 263 **RHESt as a novel plant defence mechanism**

264 We hypothesized that the ancient African cereal finger millet hosts endophytic bacteria that  
265 contribute to its resistance to *Fusarium*, a pathogenic fungal genus that has been reported to  
266 share the same African origin as its plant target. Here, we report that a microbial inhabitant of  
267 finger millet (M6) actively swarms towards invading *Fusarium* hyphae, analogous to mobile  
268 immunity cells in animals, to protect plant cells that are immobile, confirming a hypothesis that  
269 we recently proposed<sup>46</sup>. Endophyte M6 then builds a remarkable physico-chemical barrier  
270 resulting from root hair-endophyte stacking (RHESt) at the rhizosphere-root interface that  
271 prevents entry and/or traps *Fusarium* for subsequent killing. Mutant and biochemical data  
272 demonstrate that the killing activity of M6 requires genes encoding diverse regulatory factors,  
273 natural products and xenobiotic resistance. The RHESt consists of two lines of defence, a dense  
274 layer of intercalated root hairs and endophyte microcolonies followed by a long, continuous  
275 endophyte barrier layer on the root epidermal surface (see summary model, Supplementary Fig.  
276 6). RHESt represents a plant defence mechanism that has not been previously captured to the

277 best of our knowledge and is an unusual example of host-microbe symbiosis.

278

279 The epidermal root surface where microbes reside is termed the rhizoplane<sup>47-51</sup>. Soil  
280 microbes have previously been reported to form biofilm-mediated aggregates on the rhizoplane  
281<sup>52-57</sup> sometimes as part of their migration from the soil to the root endosphere<sup>48,58</sup> and may  
282 prevent pathogen entry<sup>48,59</sup>. However, here we report that an endophyte, not soil microbe, forms  
283 a pathogen barrier on the rhizoplane. The previously reported soil microbes on the rhizoplane are  
284 thought to take advantage of nutrient-rich root exudates<sup>59</sup>, whereas RHESt is a *de novo*,  
285 inducible structure that only forms in the presence of *Fusarium* in coordination with root hairs.

286

287 M6 creates its own specialized killing microhabitat by inducing growth of local root hairs  
288 which are then bent to form the RHESt scaffold, likely mediated by biofilm formation and  
289 attachment. *In vitro*, we observed that M6 synthesizes auxin (IAA), a hormone known to  
290 stimulate root hair growth<sup>60</sup> and that can be synthesized by microbes<sup>61</sup>. Root hair bending  
291 associated with RHESt might be an active process, similar to rhizobia-mediated root hair curling  
292<sup>62</sup>, or an indirect consequence of micro-colonies attachment to adjacent root hairs.

293

#### 294 **Regulatory signals within the anti-fungal pathway**

295 Some of the mutants caused pleiotropic phenotypes, including loss of swarming,  
296 attachment and/or biofilm formation, which was a surprising result. These mutants included the  
297 transcription factors associated with operons for phenazine biosynthesis, fusaric acid resistance,  
298 as well as formation of c-di-GMP. One interpretation of these results is that the underlying  
299 genes help to regulate the early steps of the anti-fungal RHESt pathway. Indeed, phenazines have

300 been reported to act as signalling molecules that regulate the expression of hundreds of genes  
301 including those responsible for motility and defense<sup>63</sup>. Our results showed an epistatic  
302 relationship between the two transcription factors regulating phenazine biosynthesis and fusaric  
303 acid resistance, with the latter required for the former (Fig. 5m,n), suggesting that the pleiotropic  
304 phenotypes observed in the fusaric acid resistance regulatory mutant may have been mediated by  
305 a reduction in phenazine signaling. Finally, c-di-GMP as a sensor of the environment and  
306 population density<sup>64,65</sup>, and a secondary messenger<sup>66</sup> involved in transcriptional regulation of  
307 genes encode virulence traits such as motility, attachment, and biofilm formation<sup>43,64,66-68</sup>, all  
308 activities that would be logically required for the RHESt-mediated anti-fungal pathway. Genome  
309 mining of strain M6 also revealed the presence of a biosynthetic cluster for 2, 3 butanediol which  
310 is a hormone known to elicit plant defences<sup>69</sup>. Production of 2, 3 butanediol was confirmed by  
311 LC-MS analysis (Supplementary Fig. 7a). Butanediol is thus a candidate signalling molecule for  
312 M6-millet cross-talk.

313

### 314 **Fungicidal compounds required for M6 killing activity**

315 In addition to RHESt formation, we gained evidence that bacterial endophyte M6 evolved  
316 multiple biochemical strategies to actively break and kill *Fusarium* hyphae (Fig. 2j and Fig. 3a,j)  
317 involving diverse classes of natural products, including phenazines, colicin V, chitinase and  
318 potentially other metabolites.

319 *Phenazines*: Phenazines are heterogeneous nitrogenous compounds produced exclusively by  
320 bacteria<sup>70</sup>. Phenazines exhibit potent antifungal activity, in particular against soil pathogens  
321 including *Fusarium* species<sup>71-73</sup>. Here M6 was observed to produce at least two distinct

322 phenazines, D-alanyl-griseolutein and griseolutein A which previously shown to have anti-  
323 microbial activities<sup>74</sup>. Phenazines lead to the accumulation of reactive oxygen species in target  
324 cells, due to their redox potential<sup>75,76</sup>. Phenazines were also reported to induce host resistance<sup>77</sup>.  
325 For bacteria to survive inside a biofilm, where oxygen diffusion is limited, molecules with high  
326 redox potential such as phenazines are required<sup>78-82</sup>. Furthermore, the redox reaction of  
327 phenazine releases extracellular DNA which enhances surface adhesion and cellular aggregation  
328 of bacteria to form a biofilm<sup>83-88</sup>. Consistent with these roles, phenazines are known to be  
329 produced inside biofilms<sup>78</sup>, and are required for biofilm formation<sup>89</sup>, which might explain the  
330 diminished biofilm formation observed with the phenazine-associated LysR mutant. Since M6  
331 was observed to produce biofilm around its fungal target (Fig. 3m) which is killed within RHESt  
332 (Fig. 2j), phenazines may be part of the killing machinery.

333 *Colicin V*: An exciting observation from this study is that colicin V also appears to be required  
334 for the fungicidal activity of strain M6 (Fig. 7). Colicin V is a small peptide antibiotic belonging  
335 to the bacteriocin family which disrupts the cell membrane of pathogens resulting in loss of  
336 membrane potential<sup>90</sup>. Bacteriocins are generally known for their antibacterial activities<sup>91</sup>.  
337 Indeed, we could find only one previous report of colicin V having anti-fungal activity<sup>92</sup>. Our  
338 results suggest that this compound may target a wider spectrum of pathogens than previously  
339 thought.

340 *Chitinase*: A Tn5 insertion in a gene (*ewc-3H2::Tn5*) encodes chitinase (EC 3.2.1.14), also  
341 resulted in a significant loss of the antifungal activity (Supplementary Fig. 5a). The mutant  
342 shows a significant reduction in production of chitinase *in vitro*, compared to wild type M6  
343 (Supplementary Fig. 7b). Chitinase exerts its antifungal activity by hydrolyzing chitin, a  
344 principle component of the fungal cell wall<sup>93,94</sup>.

345 *Other putative M6 anti-fungal metabolites:* Two additional putative Tn5 mutants suggest that  
346 other metabolites may be involved in the anti-*Fusarium* activity of strain M6 within the RHESt,  
347 specifically phenylacetic acid (PAA) and P-amino-phenyl-alanine antibiotics (PAPA). The  
348 requirement for PAA was suggested by a mutant in phenylacetic acid monooxygenase which  
349 resulted in loss of anti-*Fusarium* activity (m2D7, Supplementary Fig. 5a). This enzyme catalyzes  
350 the biosynthesis of hydroxy phenylacetic acid, derivatives of which have been shown to act as  
351 anti-fungal compounds<sup>95,96</sup>. In an earlier report, an *Enterobacter* sp. that was used to control  
352 *Fusarium* dry rot during seed storage<sup>97</sup> was shown to require phenylacetic acid, indole-3-acetic  
353 acid (IAA) and tyrosol<sup>96</sup>. In addition to PAA implicated here by the Tn5 mutant, wild type strain  
354 M6 was shown to produce IAA *in vitro* (Supplementary Fig. 4).

355 The requirement for PAPA was suggested by a putative mutant (m15A12, Supplementary Fig.  
356 5a) which disrupted a gene encoding a permease transport protein that is a part of an operon  
357 responsible for biosynthesis of PAPA and 3-hydroxy anthranilates. PAPA is the direct precursor  
358 of well known antibiotics including chloramphenicol and obaflourin<sup>98-100</sup>.

359

### 360 **M6-*Fusarium*-millet co-evolution and the fusaric acid-phenazine arms race**

361 Molecular and biochemical data suggest that the anti-fungal activity of M6 requires diverse  
362 classes of anti-fungal natural products (phenazine metabolites, colicin V peptide antibiotic,  
363 chitinase enzyme). We previously demonstrated that finger millet also hosts fungal endophytes  
364 that secrete complementary anti-*F. graminearum* natural products including polyketides and  
365 alkaloids<sup>4</sup>. These observations, combined with loss of function mutants from this study that  
366 demonstrate that no single anti-fungal mechanism is sufficient for M6 to combat *Fusarium*,

367 suggests that the endophytic community of finger millet and *Fusarium* have been engaged in a  
368 step-by-step arms race that resulted in the endophytes having a diverse weapons arsenal,  
369 presumably acting within RHESt. Consistent with this interpretation, mutant analysis showed  
370 that the anti-fungal activity of M6 requires a functional operon that encodes resistance to the  
371 *Fusarium* mycotoxin, fusaric acid. Furthermore, our results show a novel epistatic regulatory  
372 interaction between the fusaric acid resistance and phenazine pathways, wherein an M6-encoded  
373 LysR activator of fusaric acid resistance prevents fusaric acid from suppressing expression of the  
374 M6-encoded LysR regulator of phenazine biosynthesis (Fig. 5m). Fusaric acid has previously  
375 been shown to interfere with quorum sensing-mediated biosynthesis of phenazine<sup>42</sup>. We propose  
376 that the phenazine-fusaric acid arms race provides a molecular and biochemical paleontological  
377 record that M6 and *Fusarium* co-evolved.

378

379 We show how this tripartite co-evolution likely benefits subsistence farmers not only by  
380 suppressing *Fusarium* entry and hence disease in plants, but also in seeds after harvest.  
381 Specifically, under poor seed storage conditions that mimic those of subsistence farmers, M6  
382 caused dramatic reductions in contamination with DON (Fig. 1m,r), a potent human and  
383 livestock mycotoxin. Hence, in the thousands of years since ancient crop was domesticated,  
384 farmers may have been inadvertently selecting for the physico-chemical RHESt barrier activity  
385 of endophyte M6, simply by selecting healthy plants and their seeds. We have shown here that  
386 the benefits of M6 are transferable to two of the world's most important modern crops, maize  
387 and wheat (Fig. 1i,o), which are severely afflicted by *F. graminearum* and DON. In addition to  
388 *F. graminearum*, M6 inhibited the growth of five other fungi including two additional *Fusarium*  
389 species (Supplementary Table 2), suggesting that RHESt-mediated plant defence may contribute

390 to the broad spectrum pathogen resistance of finger millet reported by subsistence farmers.  
391 Despite its importance, finger millet is a scientifically neglected crop <sup>1,2</sup>. Our study suggests the  
392 value of exploring microbiome--host interactions of other scientifically neglected, ancient crops.

393

## 394 **Methods**

### 395 **Isolation, identification and antifungal activity of endophytes**

396 Finger millet seeds originating from Northern India were grown on clay Turface in the  
397 summer of 2012 according to a previously described method <sup>4</sup>. Tissue pool sets (3 sets of: 5  
398 seeds, 5 shoots and 5 root systems from pre-flowering plants) were surface sterilized following a  
399 standard protocol <sup>4</sup>. Surface sterilized tissues were ground in LB liquid medium in a sterilized  
400 mortar and pestle, then 50 µl suspensions were plated onto 3 types of agar plates (LB, Biolog  
401 Universal Growth, and PDA media). Plates were incubated at 25°C, 30°C and 37°C for 1-3 days.  
402 A total of seven bacterial colonies (M1-M7) were purified by repeated culturing on fresh media.  
403 For molecular identification of the isolated bacterial endophytes, PCR primers (Supplemental  
404 Table 7) were used to amplify and sequence 16S rDNA as previously described <sup>7</sup>, followed by  
405 best BLAST matching to GenBank. 16S rDNA sequences were deposited into GenBank.  
406 Scanning electron microscopy imaging was used to phenotype the candidate bacterium as  
407 previously described <sup>7</sup> using a Hitachi S-570 microscope (Hitachi High Technologies, Tokyo,  
408 Japan) at the Imaging Facility, Department of Food Science, University of Guelph.

409

410 To test the antifungal activity of the isolated endophytes against *F. graminearum*, agar

411 diffusion dual culture assays were undertaken in triplicate<sup>101</sup>. Nystatin (Catalog #N6261, Sigma  
412 Aldrich, USA) and Amphotericin B (Catalog #A2942, Sigma Aldrich, USA) were used as  
413 positive controls at 10 µg/ml and 5µg/ml, respectively, while the negative control was LB  
414 medium. Using a similar methodology, additional anti-fungal screening was conducted using the  
415 Fungal Type Culture Collection at Agriculture and Agrifood Canada, Guelph, ON  
416 (Supplementary Table 2).

417

## 418 **Microscopy imaging**

### 419 ***In planta* colonization of the candidate anti-fungal endophyte M6**

420 In order to verify the endophytic behaviour of the candidate anti-fungal bacterium M6 in  
421 maize, wheat and millet, the bacterium was subjected to tagging with green fluorescent protein  
422 (GFP) (vector pDSK-GFPuv)<sup>101</sup> and *in planta* visualization using confocal scanning microscopy  
423 as previously described<sup>101</sup> at the Molecular and Cellular Imaging Facility, University of Guelph,  
424 Canada.

425

### 426 ***In vitro* interaction using light microscopy**

427 Both the fungus and bacterium M6 were allowed to grow in close proximity to each other  
428 overnight on microscope slides coated with a thin layer of PDA as previously described<sup>101</sup>.  
429 Thereafter, the fungus was stained with the vitality stain, Evans blue which stains dead hyphae  
430 blue. The positive control was a commercial biological control agent (*Bacillus subtilis* QST713,  
431 Bayer CropScience, Batch # 00129001) (100 mg/10 ml). Pictures were captured using a light  
432 microscope (BX51, Olympus, Tokyo, Japan).

433 ***In vitro* and *in planta* interactions using confocal microscopy**

434 All the experiments were conducted using a Leica TCS SP5 confocal laser scanning  
435 microscope at the Molecular and Cellular Imaging Facility at the University of Guelph, Canada.

436 To visualize the interactions between endophyte M6 and *F. graminearum* inside finger  
437 millet, finger millet seeds were surface sterilized and coated with GFP-tagged endophyte, and  
438 then planted on sterile Phytigel based medium in glass tubes, each with 4-5 seeds. Phytigel  
439 medium was prepared as previously described<sup>4</sup>. At 14 days after planting, finger millet seedlings  
440 were inoculated with *F. graminearum* (50 µl of a 48 h old culture grown in potato dextrose  
441 broth) and incubated at room temperature for 24 h. The control consisted of seedlings incubated  
442 with potato dextrose broth only. There were three replicate tubes for each treatment. Thereafter,  
443 roots were stained with calcofluor florescent stain (catalog #18909, Sigma-Aldrich), which stains  
444 chitin blue, following the manufacturer's protocol, and scanned.

445

446 To visualize the attachment of bacterium M6 to fungal hyphae, GFP-tagged M6 and *F.*  
447 *graminearum* were inoculated overnight at 30°C on microscope slides covered with a thin layer  
448 of PDA. Thereafter, the fungal hyphae was stained with calcofluor and examined. The same  
449 protocol was employed to test if this recognition was disrupted in the Tn5 mutants.

450

451 To visualize biofilm formation by bacterium M6, GFP-tagged M6 were incubated on  
452 microscope slides for 24 h at 30°C. The biofilm matrix was stained with FilmTracer™ SYPRO®

453 Ruby Biofilm Matrix Stain (F10318) using the manufacturer's protocol and then examined. The  
454 same protocol was employed to test if the biofilm was disrupted in Tn5 mutants.

455

#### 456 **Suppression of *F. graminearum* in planta and accumulation in storage**

457 Bacterium M6 was tested *in planta* for its ability to suppress *F. graminearum* in two  
458 susceptible crops, maize (hybrid P35F40, Pioneer HiBred) and wheat (Quantum spring wheat,  
459 C&M Seeds, Canada), in two independent greenhouse trials as previously described for maize  
460 <sup>101</sup>, with modifications for wheat (Supplemental Method 2). ELISA analysis was conducted to  
461 test the accumulation of DON in seeds after 14 months of storage in conditions that mimic those  
462 of African subsistence farmers (temperature ~18-25°C, with a moisture content of ~40-60%) as  
463 previously described <sup>101</sup>. Control treatments consisted of plants subjected to pathogen inoculation  
464 only, and plants subjected to pathogen inoculation followed by prothioconazole fungicide  
465 spraying (PROLINE® 480 SC, Bayer Crop Science). Results were analyzed and compared using  
466 Mann-Whitney t-tests ( $P \leq 0.05$ ).

467

#### 468 **Transposon mutagenesis, gene rescues and complementation**

469 To identify the genes responsible for the antifungal activity, Tn5 transposon mutagenesis  
470 was conducted using EZ-Tn5 <R6Kγori/KAN-2>Tnp Transposome™ kit (catalog #TSM08KR,  
471 Epicentre, Madison, USA) according to the manufacturer's protocol. The mutants were screened  
472 for loss of anti-*Fusarium* activity using the agar dual culture method compared to wild type.  
473 Insertion mutants that completely lost the antifungal activity *in vitro* were further tested for loss

474 of *in planta* activity using maize as a model in two independent greenhouse trials (same protocol  
475 as described above). The sequences flanking each candidate Tn5 insertion mutant of interest  
476 were identified using plasmid rescues according to the manufacturer's protocol (Supplemental  
477 Method 3). The rescued gene sequences were BLAST searched against the whole genome  
478 sequence of bacterium M6<sup>26</sup>. To test if the candidate genes are inducible by *F. graminearum* or  
479 constitutively expressed, real-time PCR analysis was conducted using gene specific primers  
480 (Supplemental Method 4). Operons were tentatively predicted using FGENESB<sup>102</sup> from  
481 Softberry Inc. (USA). Promoter regions were predicted using PePPER software (University of  
482 Groningen, The Netherlands)<sup>103</sup>. In order to confirm the identity of the genes discovered by Tn5  
483 mutagenesis, each mutant was complemented with the corresponding predicted wild type coding  
484 sequence which was synthesized (VectorBuilder, Cyagen Biosciences, USA) using a pPR322  
485 vector backbone (Novagen) under the control of the T7 promoter. Two microlitres of each  
486 synthesized vector was electroporated using 40 µl electro competent cells of the corresponding  
487 mutant. The transformed bacterium cells were screened for gain of the antifungal activity against  
488 *F. graminearum* using the dual culture assay as described above.

489

## 490 **Mutant phenotyping**

491 *Transmission electron microscopy (TEM)*: To phenotype the candidate mutants, TEM imaging  
492 was conducted. Wild type strain M6 and each of the candidate mutants were cultured overnight  
493 in LB medium (37°C, 250 rpm). Thereafter, 5 µl of each culture were pipetted onto a 200-mesh  
494 copper grid coated with carbon. The excess fluid was removed onto a filter, and the grid was  
495 stained with 2% uranyl acetate for 10 sec. Images were taken by a F20 G2 FEI Tecnai

496 microscope operating at 200 kV equipped with a Gatan 4K CCD camera and Digital Micrograph  
497 software at the Electron Microscopy Unit, University of Guelph, Canada.

498

499 *Motility assay:* Wild type or mutant strains were cultured overnight in LB medium (37°C, 225  
500 rpm). The OD<sub>595</sub> for each culture was adjusted to 1.0, then 15 µl of each culture were spotted on  
501 the center of a semisolid LB plates (0.3% agar) and incubated overnight (37°C, no shaking).  
502 Motility was measured as the diameter of the resulting colony. There were ten replicates for each  
503 culture. The entire experiment was repeated independently.

504

505 *Swarming test:* To examine the ability of the strains to swarm and form colonies around the  
506 fungal pathogen, *in vitro* interaction/light microscopy imaging was conducted. Wild type M6 and  
507 each mutant were incubated with *F. graminearum* on microscope slides covered with PDA (as  
508 described above). *F. graminearum* hyphae was stained with lactophenol blue solution (catalog  
509 #61335, Sigma-Aldrich) then examined under a light microscope (B1372, Axiophot, Zeiss,  
510 Germany) using Northern Eclipse software.

511

512 *Biofilm spectroscopic assay:* To test the ability of the strains to form biofilms, the strains were  
513 initially cultured overnight in LB medium (37°C and 250 rpm), and adjusted to OD<sub>600</sub> of 0.5.  
514 Cultures were diluted in LB (1:100), thereafter, 200 µl from each culture were transferred to a 96  
515 well microtitre plate (3370, Corning Life Sciences, USA) in 6 replicates. The negative control  
516 was LB medium only. The microtitre plate was incubated for 2 days at 37°C. The plate was

517 emptied by aspiration and washed three times with sterile saline solution. Adherent cells were  
518 fixed with 200  $\mu$ l of 99% methanol for 15 min then air dried. Thereafter, 200  $\mu$ l of 2% crystal  
519 violet (94448, Sigma) were added to each well for 5 min then washed with water, and left to air  
520 dry. Finally, 160  $\mu$ l of 33% (v/v) glacial acetic acid were added to each well to solubilise the  
521 crystal violet stain. The light absorption was read by a spectrophotometer (SpectraMax plus 348  
522 microplate reader, Molecular Devices, USA) at 570 nm<sup>104</sup>. The entire experiment was repeated  
523 independently.

524

525 *Fusaric acid resistance:* To test the ability of M6 wild type or *EwfR::Tn5* to resist fusaric acid,  
526 the strains were allowed to grow on LB agar medium supplemented with different concentrations  
527 of fusaric acid (0.01, 0.05 and 0.1%, catalog #F6513, Sigma Aldrich) as previously reported<sup>105</sup>.

528

529 *c-di-GMP chemical complementation:* To test if the Tn5 insertion in the predicted guanylate  
530 cyclase gene could be complemented by exogenous c-di-GMP, M6 wild type or *EwgC::Tn5*  
531 strains were grown on LB agar medium supplemented with c-di-GMP (0.01 or 0.02 mg/ml)  
532 (Catalogue # TLRL-CDG, Cedarlane). After 24 h, the agar diffusion method was used to test for  
533 antifungal activity.

534

535 *Colicin V assay:* To verify that the Tn5 insertion in the predicted colicin V production gene  
536 caused loss of colicin V secretion, M6 wild type or *EwvC-4B9::Tn5* strains were inoculated as

537 liquid cultures ( $OD_{600} = 0.5$ ) into holes created in LB agar medium pre-inoculated after cooling  
538 with an *E.coli* strain sensitive to colicin V (MC4100, ATCC 35695)<sup>90</sup>.

539

#### 540 **Biochemical and enzymatic assays**

541 *Detection of anti-fungal phenazine derivatives:* For phenazine detection, bio-guided fractionation  
542 combined with LC-MS analysis was undertaken. Wild type M6 or mutant bacterial strains were  
543 grown for 48 h on Katznelson and Lochhead liquid medium<sup>106</sup>, harvested by freeze drying, then  
544 the lyophilized powder from each strain was extracted by methanol. The methanolic extracts  
545 were tested for anti-*Fusarium* activity using the agar diffusion method as described above. The  
546 extracts were dried under vacuum and dissolved in a mixture of water and acetonitrile then  
547 fractionized over a preparative HPLC C18 column (Nova-Pak HR C18 Prep Column, 6  $\mu$ m, 60  
548 Å, 25 x 100 mm prepack cartridge, part # WAT038510, Serial No 0042143081sp, Waters Ltd,  
549 USA). The solvent system consisted of purified water (Nanopure, USA) and acetonitrile (starting  
550 at 99:1 and ending at 0:100) pumped at a rate of 5 ml/min. The eluted peaks were tested for anti-  
551 *Fusarium* activity. Active fractions were subjected to LC-MS analysis. Each of the active  
552 fractions was run on a Luna C18 column (Phenomenex Inc, USA) with a gradient of 0.1% formic  
553 acid in water and 0.1% formic in acetonitrile. Peaks were analyzed by mass spectroscopy  
554 (Agilent 6340 Ion Trap), ESI, positive ion mode. LC-MS analysis was conducted at the Mass  
555 Spectroscopy Facility, McMaster University, ON, Canada.

556

557 *GC-MS to detect production of 2,3 butanediol:* To detect 2,3 butanediol, wild type strain M6 was  
558 grown for 48 h on LB medium. The culture filtrate was analyzed by GC-MS (Mass Spectroscopy

559 Facility, McMaster University, ON, Canada) and the resulting peaks were analyzed by searches  
560 against the NIST 2008 database.

561

562 *Chitinase assay:* Chitinase activity of wild type strain M6 and the putative chitinase Tn5 mutant  
563 was assessed using a standard spectrophotometric assay employing the Chitinase Assay Kit  
564 (catalog #CS0980, Sigma Aldrich, USA) according to the manufacturer's protocol. There were  
565 three replicates for each culture, and the entire experiment was repeated independently.

566

## 567 **Figures legends**

568 **Figure 1| Isolation, identification and antifungal activity of endophytes. a,** Picture showing  
569 finger millet grain head. **b,** Mixed culture of endophytes isolated from finger millet. **c,**  
570 Quantification of the inhibitory effect of finger millet endophytes or fungicide controls on the  
571 growth of *F. graminearum in vitro*. For these experiments, n=3. **d,** M6 endophyte suppresses the  
572 growth of *F. graminearum* hyphae (white) using the dual culture method. **e,** Imaging of M6  
573 viewed by scanning electron microscopy. **f-g,** GFP-tagged M6 inside roots of finger millet  
574 viewed by scanning confocal microscopy. **h,** GFP-tagged M6 inside roots of maize (stained with  
575 propidium iodide). **i,** Effect of M6 treatment on suppression of *F. graminearum* disease in maize  
576 in two greenhouse trials. **j-l,** (left to right) Representative ears from M6, fungicide and *Fusarium*  
577 only treatments. **m,** Effect of M6 or controls on reducing DON mycotoxin contamination in  
578 maize during storage following the two greenhouse trials. **n,** GFP-tagged M6 inside roots of  
579 wheat viewed by confocal microscopy. **o,** Effect of M6 treatment on suppression of *F.*  
580 *graminearum* disease in wheat in two greenhouse trials. **p,** Picture of a healthy wheat grain. **q,**

581 Picture of an infected wheat grain. **r**, Effect of M6 or controls on reducing DON mycotoxin  
582 contamination in wheat during storage following the two greenhouse trials. Scale bars in all  
583 pictures equal 5  $\mu\text{m}$ . For greenhouse disease trials, n=20 for M6 and n=10 for the controls. For  
584 DON quantification, n=3 pools of seeds. The whiskers (**i**, **o**) indicate the range of data points.  
585 The error bars (**c**, **m**, **q**) indicate the standard error of the mean. For all graphs, letters that are  
586 different from one another indicate that their means are statistically different ( $P \leq 0.05$ ).

587

588 **Figure 2| Confocal imaging of m6-*fusarium* interactions in finger millet roots.** **a**, Picture of  
589 millet seedling showing primary root (PR) zone used for confocal microscopy. **b**, Control  
590 primary root that was seed coated with GFP-M6 (green) but not infected with *F. graminearum*.  
591 As a control, the tissue was stained with fungal stain calcofluor to exclude the presence of other  
592 fungi. Root following seed coating with GFP-tagged endophyte M6 (M6, green) following  
593 inoculation with *F. graminearum* (Fg, purple blue, calcofluor stained) showing interactions with  
594 root hairs (RH, magenta, lignin autofluorescence). **c-d**, Low (**c**) and high (**d**) magnifications to  
595 show the dense root hair and endophyte barrier layers. **e-f**, Low (**e**) and high (**f**) magnifications at  
596 the edge of the barrier layers. **g-h**, Low (**g**) and high (**h**) magnifications in a deeper confocal  
597 plane of the root hair layer shown in (**d**) showing root hair endophyte stacking (RHESt) with  
598 trapped fungal hyphae. **i-j**, Low (**i**) and high (**j**) magnifications of the interactions between M6  
599 (green) and *F. graminearum* in the absence of root hair-lignin autofluorescence, showing  
600 breakage of fungal hyphae.

601

602 **Figure 3| Behavior and interactions of endophyte m6 and *f. graminearum* in vitro on**  
603 **microscope slides. a-c**, Light microscopy of interactions between *F. graminearum* (Fg) and M6  
604 following staining with Evans blue, which stains dead hyphae blue. Shown are (a) Fg following  
605 overnight co-incubation with M6, (b) Fg, grown away from M6 (control), and (c) Fg following  
606 overnight co-incubation with a commercial biological control agent. **d-i**, Time course to  
607 illustrate the swarming and attachment behaviour of GFP-tagged M6 (green) to Fg (blue,  
608 calcofluor stained) viewed at 0.5 h, 1.5 h, 3 h, 6 h, 6 h (close-up) and 8 h following co-  
609 incubation, respectively. Fg and M6 shown in (d) and (e) were inoculated on the same slide  
610 distal from one another at the start of the time course but digitally placed together for these  
611 illustrations. **j**, M6 shown breaking Fg hypha. **k**, Transmission electron microscope picture of  
612 M6 showing its characteristic flagella. **(l-m)** Biofilm formed by M6 as viewed by staining with  
613 Ruby film tracer (red) in the (l) absence of Fg or (m) presence of Fg.

614

615 **Figure 4 | Characterization of phenazine mutant *ewpR-5D7::Tn5*. a**, Effect of M6 mutant  
616 strain *ewpR* on suppression of *F. graminearum* (Fg) in maize compared to wild type M6 and Fg-  
617 only control, with corresponding, representative maize ear pictures. **b**, Genomic organization of  
618 the predicted phenazine biosynthetic operon showing the position of the Tn5 insertion and  
619 putative LysR binding site within the promoter (P). **c**, Quantitative real time PCR (qRT-PCR)  
620 gene expression of the two core phenazine genes (*ewpF1* and *ewpF2*) in wild type M6 (+) and  
621 the mutant (-) (*ewpR*). **d**, Illustration of the phenazine biosynthetic pathway. **e**, Agar diffusion  
622 assay showing the inhibitory effect of different methanol extracts on the growth of Fg from wild  
623 type M6, two wild type fractions (FrA, FrB), the *ewpR* mutant (mutant), a random Tn5 insertion  
624 or buffer. **f-g**, Mass spectroscopy analysis of putative phenazine derivatives in wild type M6

625 fractions A and B. **h**, Quantification of *ewpR*<sup>-</sup> mutant strain (M) motility compared to wild type  
626 M6 (W), with representative pictures (inset) of motility assays on semisolid agar plates. **i-j**, Light  
627 microscopy image showing loss of swarming and colony formation of (**i**) *ewpR*<sup>-</sup> mutant strain  
628 around Fg hyphae stained with lactophenol blue, compared to (**j**) wild type M6. **k**, Electron  
629 microscopy image of *ewpR*<sup>-</sup> mutant strain. **l**, Confocal microscopy image showing attachment  
630 pattern of GFP-tagged *ewpR*<sup>-</sup> mutant strain (green) to Fg hyphae stained with calcofluor stain,  
631 compared to wild type M6 (inset). **m**, Confocal microscopy image showing reduced  
632 proteinaceous biofilm matrix stained with Ruby film tracer (red) associated with GFP-tagged  
633 *ewpR*<sup>-</sup> mutant strain compared to wild type M6 (inset). **n**, Spectrophotometric quantification of  
634 biofilm formation associated with wild type M6 compared to the *ewpR*<sup>-</sup> mutant strain, with  
635 representative biofilm assay well pictures (left and right, respectively; 3 replicates shown). For  
636 graphs shown in (**a**, **c**, **h**, **n**) letters that are different from one another indicate that their means  
637 are statistically different ( $P \leq 0.05$ ), and the whiskers represent the standard error of the mean.

638

639 **Figure 5 | Characterization of fusaric acid resistance mutant *ewfR*-7D5::Tn5.** **a**, Genomic  
640 organization of the predicted fusaric acid resistance operon showing the position of the Tn5  
641 insertion and putative LysR binding site within the promoter (P). **b-c**, The inhibitory effect of  
642 fusaric acid embedded within agar on the growth of the *ewfR*<sup>-</sup> mutant compared to wild type M6.  
643 **d**, Quantitative real time PCR gene expression of two protein-coding genes required for the  
644 formation of the fusaric acid efflux pump (*ewfD* and *ewfE*) in wild type M6 (+) and the mutant (-  
645 ) (*ewfR*<sup>-</sup>). **e**, Quantification of *ewfR*<sup>-</sup> mutant strain (M) motility compared to wild type M6 (W),  
646 with representative pictures (inset) of motility assays on semisolid agar plates. **f-g**, Light  
647 microscopy image showing decreased swarming and colony formation of (**f**) the *ewfR*<sup>-</sup> mutant

648 strain around Fg hyphae stained with lactophenol blue, compared to (g) wild type M6. h,  
649 Electron microscopy image of the *ewfR*<sup>-</sup> mutant strain. i, Confocal microscopy image showing  
650 the attachment pattern of the GFP-tagged *ewfR*<sup>-</sup> mutant strain (green) to Fg hyphae stained with  
651 calcofluor stain, compared to wild type M6 (inset). j, Confocal microscopy image showing a  
652 proteinaceous biofilm matrix stained with Ruby film tracer (red) associated with GFP-tagged  
653 *ewfR*<sup>-</sup> mutant strain compared to wild type M6 (inset). k, Spectrophotometric quantification of  
654 biofilm formation associated with wild type M6 compared to the *ewfR*<sup>-</sup> mutant strain, with  
655 representative biofilm assay well pictures (left and right, respectively; 3 replicates shown). qRT-  
656 PCR analysis of: (l) wild type *ewfR* expression in a wild type M6 background, (m) wild type  
657 *ewpR* in an *ewfR*<sup>-</sup> mutant background, and (n) wild type *ewpR* in a wild type M6 background.  
658 For graphs shown in (d, e, k, l- n) letters that are different from one another indicate that their  
659 means are statistically different ( $P \leq 0.05$ ; in the case of l-n, within a time point), and the whiskers  
660 represent the standard error of the mean.

661

662 **Figure 6 | Characterization of di-guanylate cyclase mutant *ewgS-10A8::Tn5*.** a, Illustration  
663 of the enzymatic conversion of 2 guanosine phosphate to c-di-GMP catalyzed by di-guanylate  
664 cyclase. b, Complementation of the putative *ewgS*<sup>-</sup> mutant with respect to inhibition of *F.*  
665 *graminearum* (Fg) by addition of c-di-GMP (0.01 and 0.02 mg/ml), compared to wild type strain  
666 M6. c, qRT-PCR analysis of wild type *ewgS* expression in a wild type M6 background. d,  
667 Quantification of *ewgS*<sup>-</sup> mutant strain (M) motility compared to wild type M6 (W), with  
668 representative pictures (inset) of motility assays on semisolid agar plates. e-f, Light microscopy  
669 image showing decrease in swarming and colony formation of (e) *ewgS*<sup>-</sup> mutant strain around Fg  
670 hyphae stained with lactophenol blue, compared to (f) wild type M6. g, Electron microscopy

671 image of *ewgS*<sup>-</sup> mutant strain. **h**, Confocal microscopy image showing attachment pattern of  
672 GFP-tagged *ewgS*<sup>-</sup> mutant strain (green) to Fg hyphae stained with calcofluor stain, compared to  
673 wild type M6 (inset). **i**, Confocal microscopy image showing loss of proteinaceous biofilm  
674 matrix stained with Ruby film tracer (red) associated with GFP-tagged *ewgS*<sup>-</sup> mutant strain  
675 compared to wild type M6 (inset). **j**, Spectrophotometric quantification of biofilm formation  
676 associated with wild type M6 compared to the *ewgS*<sup>-</sup> mutant strain, with representative biofilm  
677 assay well pictures (left and right, respectively; 3 replicates shown). For graphs shown in (**c**, **d**, **j**)  
678 letters that are different from one another indicate that their means are statistically different  
679 ( $P \leq 0.05$ ), and the whiskers represent the standard error of the mean.

680

681 **Figure 7 | Characterization of Colicin V Mutant *ewvC*-4B9::Tn5.** **a**, Dual culture agar  
682 diffusion assay showing loss of antagonism against the colicin V sensitive *E coli* strain  
683 (MC4100) by the *ewvC* mutant compared to wild type M6. **b**, qRT-PCR analysis of wild type  
684 *ewvC* expression in a wild type M6 background. **c**, Quantification of *ewvC* mutant strain (M)  
685 motility compared to wild type M6 (W), with representative pictures (inset) of motility assays on  
686 semisolid agar plates. **d-e**, Light microscopy image showing decrease in swarming and colony  
687 formation of (**d**) the *ewvC* mutant strain around Fg hyphae stained with lactophenol blue,  
688 compared to (**e**) wild type M6. **f**, Electron microscopy image of the *ewvC* mutant strain. **g**,  
689 Confocal microscopy image showing the attachment pattern of the GFP-tagged *ewvC* mutant  
690 strain (green) to Fg hyphae stained with calcofluor stain, compared to wild type M6 (inset). **h**,  
691 Confocal microscopy image showing the proteinaceous biofilm matrix stained with Ruby film  
692 tracer (red) associated with the GFP-tagged *ewvC* mutant strain compared to wild type M6  
693 (inset). **i**, Spectrophotometric quantification of biofilm formation associated with wild type M6

694 compared to the *ewvC* mutant strain, with representative biofilm assay well pictures (left and  
695 right, respectively; 3 replicates shown). For graphs shown in **(b, c, i)** letters that are different  
696 from one another indicate that their means are statistically different ( $P \leq 0.05$ ), and the whiskers  
697 represent the standard error of the mean.

698

## 699 **Supplementary Data**

700 **Supplementary Table 1 | Taxonomic classification of finger millet bacterial endophytes**  
701 **based on 16S rDNA sequences and BLAST Analysis.**

702

703 **Supplementary Table 2 | Effect of endophyte strain M6 isolated from finger millet on the**  
704 **growth of diverse fungal pathogens *in vitro*.**

705

706 **Supplementary Table 3 | Suppression of *F. graminearum* disease symptoms in maize and**  
707 **wheat by endophyte M6 in replicated greenhouse trials.**

708

709 **Supplementary Table 4 | Reduction of DON mycotoxin accumulation during prolonged**  
710 **seed storage following treatment with endophyte M6.**

711

712 **Supplementary Table 5 | Complete list of strain M6 Tn5 insertion mutants showing loss of**  
713 **antifungal activity against *F. graminearum* in vitro.**

714

715 **Supplementary Table 6 | M6 wild type nucleotide coding sequences<sup>26</sup> corresponding to Tn5**  
716 **insertion mutants that showed loss of antifungal activity against *F. graminearum* in vitro.**

717

718 **Supplementary Table 7 | Gene-specific primers used in quantitative real-time PCR analysis**  
719 **(see Supplemental Methods).**

720

721 **Supplementary Figure 1 | 16S rDNA based phylogenetic tree of finger millet endophytes**  
722 **M1-M7.**

723

724 **Supplementary Figure 2 | Image of finger millet seedlings previously seed-coated with**  
725 **GFP-tagged M6 showing no pathogenic symptoms, consistent with the strain behaving as**  
726 **an endophyte.**

727

728 **Supplementary Figure 3 | Suppression of *F. graminearum* (Fg) by M6 and its effect on**  
729 **grain yield in greenhouse trials. a-b, Effect of endophyte M6 on grain yield per plant in two**  
730 **greenhouse trials for (a) maize and (b) wheat. c, Effect of treatment with endophyte M6 on Fg**  
731 **disease symptoms in maize ears when the endophyte was applied as a seed coat or foliar spray**

732 compared to a *Fusarium* only control treatment. Letters that are different from one another  
733 within a trial indicate that their means are statistically different ( $P \leq 0.05$ ). The whiskers indicate  
734 the range of data.

735

736 **Supplementary Figure 4 | Assay for production of indole-3-acetic acid (IAA, auxin) by wild**  
737 **type strain M6.** Production of indole-3-acetic acid (IAA) *in vitro* by wild type strain M6  
738 compared to a positive control (bacterial endophyte strain E10)<sup>107</sup> using the Salkowski reagent  
739 colorimetric assay.

740

741 **Supplementary Figure 5 | Tn5 mutagenesis-mediated discovery, validation and**  
742 **complementation of genes required for the anti-*Fusarium* activity of strain M6.** **a**, Loss of  
743 anti-*F. graminearum* activity associated with each Tn5 insertion mutant using the *in vitro* dual  
744 culture diffusion assay, along with a representative image (inset) of the mutant screen. **b-c**, *In*  
745 *planta* validation of loss of anti-fungal activity of M6 mutant strains based on quantification of  
746 *F. graminearum* disease symptoms on maize ears, in **(b)** greenhouse trial 1, and **(c)** greenhouse  
747 trial 2. Only mutant strains that completely lost anti-fungal activity *in vitro* were selected for *in*  
748 *planta* validation. The whiskers indicate the range of data points. Letters that are different from  
749 one another indicate that their means are statistically different ( $P \leq 0.05$ ). **d**, Genetic  
750 complementation of Tn5 mutants with the predicted, corresponding wild type coding sequences.  
751 Shown are representative images.

752

753 **Supplementary Figure 6 | Model to illustrate the interaction between strain M6, the host**  
754 **plant and *F. graminearum* pathogen.** Following pathogen sensing, M6 swarm towards  
755 *Fusarium* hyphae and induces local hair growth, perhaps mediated by M6-IAA production. M6  
756 then forms microcolony stacks between the elongated and bent root hairs resulting root hair-  
757 endophyte stack (RHESt) formation, likely mediated by biofilms. The RHESt formation  
758 prevents entry and/or traps *F. graminearum* for subsequent killing. M6 killing requires diverse  
759 antimicrobial compounds including phenazines. *Fusarium* will produce fusaric acid which  
760 interferes with phenazine biosynthesis. However, M6 has a specialized fusaric acid-resistance  
761 pump system which is predicted to pump the mycotoxin outside the endophyte cell.

762

763 **Supplementary Figure 7 | Assays for production of butanediol and chitinase by strain M6.**  
764 **a,** Entire GC chromatogram showing an arrow pointing to a peak with RT 11.13 with a  
765 molecular weight and fragmentation pattern (inset) that matches 2, 3 butanediol when searched  
766 against the NIST 2008 database. **b,** Quantification of chitinase production by an M6 mutant  
767 strain carrying a Tn5 insertion in a chitinase encoding gene (*ewc-3H2::Tn5*) compared to wild  
768 type M6 (see Supplementary Table 7).

769

## 770 **Conflict of Interest Statement**

771 The authors declare that they have no competing financial interests.

772

## 773 **Author Contributions**

774 WKM designed and conducted all experiments, analyzed all data and wrote the manuscript. CS  
775 assisted in the greenhouse trials. VLR performed the DON quantification experiments. CE and  
776 JE sequenced the M6 genome and provided gene annotations. MNR helped to design the  
777 experiments and edited the manuscript. All authors read and approved the manuscript.

778

## 779 **Acknowledgements**

780 We are very thankful to Dr. Michaela Streuder (Department of Molecular and Cellular Biology,  
781 University of Guelph) for assistance in confocal microscopy experiments and for her insightful  
782 comments. We thank Prof. A. Schaafsma and Dr. Ljiljana Tamburic-Ilincic (Ridgetown College,  
783 University of Guelph, Canada) for kindly providing hybrid maize and wheat seeds, respectively.  
784 We thank Marina Atalla for assistance in disease scoring. WKM was supported by generous  
785 scholarships from the Government of Egypt and the University of Guelph (International  
786 Graduate Student Scholarships, 2012, 2014). This research was supported by grants to MNR by  
787 the Ontario Ministry of Agriculture, Food and Rural Affairs (OMAFRA), Grain Farmers of  
788 Ontario (GFO), Natural Sciences and Engineering Research Council of Canada (NSERC) and  
789 the CIFSRF program funded by the International Development Research Centre (IDRC, Ottawa)  
790 and Canadian Department of Global Affairs.

791

## 792 **References**

- 793 1 Goron, T. L. & Raizada, M. N. Genetic diversity and genomic resources available for the small  
794 millet crops to accelerate a New Green Revolution. *Front. Plant Sci.* **6**, 157 (2015).  
795  
796 2 Thilakarathna, M. S. & Raizada, M. N. A review of nutrient management studies involving finger  
797 millet in the semi-arid tropics of Asia and Africa. *Agronomy* **5**, 262-290 (2015).

- 798  
799 3 Hilu, K. W. & de Wet, J. M. J. Domestication of *Eleusine coracana*. *Econ. Bot.* **30**, 199-208 (1976).  
800  
801 4 Mousa, W. K. *et al.* An endophytic fungus isolated from finger millet (*Eleusine coracana*) produces  
802 anti-fungal natural products. *Front. Microbiol.* **6**, 1157(2015).  
803  
804 5 Sundaramari, P. V. a. M. Rationality and adoption of indigenous cultivation practices of finger millet  
805 (*Eleusine coracana* (L.) Gaertn.) by the tribal farmers of Tamil Nadu. *Intl. J. Manag. Social Sci.* **02**,  
806 970-977 (2015).  
807  
808 6 Sutton, J. C. Epidemiology of wheat head blight and maize ear rot caused by *Fusarium*  
809 *graminearum*. *Can. J. Plant Pathol.* **4**, 195-209 (1982).  
810  
811 7 Mousa, W. K., Shearer, C., Limay-Rios, V., Zhou, T. & Raizada, M. N. Bacterial endophytes from  
812 wild maize suppress *Fusarium graminearum* in modern maize and inhibit mycotoxin accumulation.  
813 *Front. Plant Sci.* **6**, 805 (2015).  
814  
815 8 Munimbazi, C. & Bullerman, L. B. Molds and mycotoxins in foods from Burundi. *J. Food Prot.* **59**,  
816 869-875 (1996).  
817  
818 9 Chandrashekar, A. & Satyanarayana, K. Disease and pest resistance in grains of sorghum and  
819 millets. *J. Cereal Sci.* **44**, 287-304 (2006).  
820  
821 10 Siwela, M., Taylor, J., de Milliano, W. A. & Duodu, K. G. Influence of phenolics in finger millet on  
822 grain and malt fungal load, and malt quality. *Food Chem.* **121**, 443-449 (2010).  
823  
824 11 Wilson, D. Endophyte: the evolution of a term, and clarification of its use and definition. *Oikos* **73**,  
825 274-276 (1995).  
826  
827 12 Johnston-Monje, D. & Raizada, M. N. Conservation and diversity of seed associated endophytes in  
828 across boundaries of evolution, ethnography and ecology. *PLoS ONE* **6**, e20396, (2011).  
829  
830 13 Waller, F. *et al.* The endophytic fungus *Piriformospora indica* reprograms barley to salt-stress  
831 tolerance, disease resistance, and higher yield. *Proc. Natl. Acad. Sci. (USA)* **102**, 13386-13391,  
832 (2005).  
833  
834 14 Haas, D. & Defago, G. Biological control of soil-borne pathogens by fluorescent pseudomonads.  
835 *Nat. Rev. Microbiol.* **3**, 307-319 (2005).  
836  
837 15 Mousa, W. K. & Raizada, M. N. The diversity of anti-microbial secondary metabolites produced by  
838 fungal endophytes: An interdisciplinary perspective. *Front. Microbiol.* **4**,65 (2013).  
839  
840 16 Mousa, W. K. & Raizada, M. N. Biodiversity of genes encoding anti-microbial traits within plant  
841 associated microbes. *Front. Plant Sci.* **6**, 231(2015).  
842  
843 17 O'Donnell, K. *et al.* Phylogenetic analyses of RPB1 and RPB2 support a middle Cretaceous origin  
844 for a clade comprising all agriculturally and medically important fusaria. *Fungal Genet. Biol.* **52**, 20-  
845 31 (2013).  
846  
847 18 Saleh, A. A., Esele, J., Logrieco, A., Ritieni, A. & Leslie, J. F. *Fusarium verticillioides* from finger  
848 millet in Uganda. *Food Addit. Contam.* **29**, 1762-1769 (2012).

- 849  
850 19 Pall, B. & Lakhani, J. Seed mycoflora of ragi, *Eleusine coracana* (L.) Gaertn. *Res. Develop. Rep.* **8**,  
851 78-79 (1991).  
852  
853 20 Amata, R. *et al.* An emended description of *Fusarium brevicatenulatum* and *F. pseudoanthophilum*  
854 based on isolates recovered from millet in Kenya. *Fungal Divers.* **43**, 11-25 (2010).  
855  
856 21 Penugonda, S., Girisham, S. & Reddy, S. Elaboration of mycotoxins by seed-borne fungi of finger  
857 millet (*Eleusine coracana* L.). *Intl. J. Biotech. Mol. Biol. Res.* **1**, 62-64 (2010).  
858  
859 22 Ramana, M. V., Nayaka, S. C., Balakrishna, K., Murali, H. & Batra, H. A novel PCR–DNA probe  
860 for the detection of fumonisin-producing *Fusarium* species from major food crops grown in southern  
861 India. *Mycology* **3**, 167-174 (2012).  
862  
863 23 Adipala, E. Seed-borne fungi of finger millet. *E. Afr. Agricult. Forest. J.* **57**, 173-176 (1992).  
864  
865 24 Dereeper, A. *et al.* Phylogeny. fr: robust phylogenetic analysis for the non-specialist. *Nucleic acids*  
866 *Res.* **36**, 465-469 (2008).  
867  
868 25 Dereeper, A., Audic, S., Claverie, J.-M. & Blanc, G. BLAST-explorer helps you building datasets for  
869 phylogenetic analysis. *BMC Evol. Biol.* **10**, 8 (2010).  
870  
871 26 Ettinger, C. L., Mousa, W. M., Raizada, M. N. & Eisen, J. A. Draft Genome Sequence of  
872 *Enterobacter* sp. Strain UCD-UG\_FMILLET (Phylum Proteobacteria). *Genome Announc.* **3**, e0146-  
873 14 (2015).  
874  
875 27 Chongo, G. *et al.* Reaction of seedling roots of 14 crop species to *Fusarium graminearum* from  
876 wheat heads. *Can. J. Plant Pathol.* **23**, 132-137 (2001).  
877  
878 28 Pitts, R. J., Cernac, A. & Estelle, M. Auxin and ethylene promote root hair elongation in  
879 *Arabidopsis*. *Plant J.* **16**, 553-560 (1998).  
880  
881 29 Parsons, J. F. *et al.* Structure and function of the phenazine biosynthesis protein PhzF from  
882 *Pseudomonas fluorescens* 2-79. *Biochemistry* **43**, 12427-12435 (2004).  
883  
884 30 Lu, J. *et al.* LysR family transcriptional regulator PqsR as repressor of pyoluteorin biosynthesis and  
885 activator of phenazine-1-carboxylic acid biosynthesis in *Pseudomonas* sp. M18. *J. Biotechnol.* **143**,  
886 1-9 (2009).  
887  
888 31 Goethals, K., Van Montagu, M. & Holsters, M. Conserved motifs in a divergent nod box of  
889 *Azorhizobium caulinodans* ORS571 reveal a common structure in promoters regulated by LysR-type  
890 proteins. *Proc. Natl. Acad. Sci. (USA)* **89**, 1646-1650 (1992).  
891  
892 32 Wang, Y., Luo, Q., Zhang, X. & Wang, W. Isolation and purification of a modified phenazine,  
893 griseoluteic acid, produced by *Streptomyces griseoluteus* P510. *Res. Microbiol.* **162**, 311-319,  
894 (2011).  
895  
896 33 Nakamura, S., Wang, E. L., Murase, M., Maeda, K. & Umezawa, H. Structure of griseolutein A. *J.*  
897 *Antibiot.* **12**, 55-58 (1959).  
898

- 899 34 Giddens, S. R., Feng, Y. & Mahanty, H. K. Characterization of a novel phenazine antibiotic gene  
900 cluster in *Erwinia herbicola* Eh1087. *Mol. Microbiol.* **45**, 769-783 (2002).  
901
- 902 35 Kitahara, M. *et al.* Saphenamycin, a novel antibiotic from a strain of *Streptomyces*. *J. Antibiot.* **35**,  
903 1412-1414 (1982).  
904
- 905 36 Toyoda, H., Katsuragi, K., Tamai, T. & Ouchi, S. DNA Sequence of genes for detoxification of  
906 fusaric acid, a wilt-inducing agent produced by *Fusarium* species. *J. Phytopathol.* **133**, 265-277  
907 (1991).  
908
- 909 37 Utsumi, R. *et al.* Molecular cloning and characterization of the fusaric acid-resistance gene from  
910 *Pseudomonas cepacia*. *Agri. Biol. Chem.* **55**, 1913-1918 (1991).  
911
- 912 38 Marre, M., Vergani, P. & Albergoni, F. Relationship between fusaric acid uptake and its binding to  
913 cell structures by leaves of *Egeria densa* and its toxic effects on membrane permeability and  
914 respiration. *Physiol. Mol. Plant Pathol.* **42**, 141-157 (1993).  
915
- 916 39 Bacon, C., Hinton, D. & Hinton, A. Growth-inhibiting effects of concentrations of fusaric acid on the  
917 growth of *Bacillus mojavensis* and other biocontrol *Bacillus* species. *J. App. Microbiol.* **100**, 185-194  
918 (2006).  
919
- 920 40 Borges-Walmsley, M., McKeegan, K. & Walmsley, A. Structure and function of efflux pumps that  
921 confer resistance to drugs. *Biochem. J.* **376**, 313-338 (2003).  
922
- 923 41 Hu, R.-M., Liao, S.-T., Huang, C.-C., Huang, Y.-W. & Yang, T.-C. An inducible fusaric acid  
924 tripartite efflux pump contributes to the fusaric acid resistance in *Stenotrophomonas maltophilia*.  
925 *PLoS ONE* **7**, e51053 (2012).  
926
- 927 42 van Rij, E. T., Girard, G., Lugtenberg, B. J. & Bloemberg, G. V. Influence of fusaric acid on  
928 phenazine-1-carboxamide synthesis and gene expression of *Pseudomonas chlororaphis* strain  
929 PCL1391. *Microbiology* **151**, 2805-2814 (2005).  
930
- 931 43 Römling, U., Galperin, M. Y. & Gomelsky, M. Cyclic di-GMP: the first 25 years of a universal  
932 bacterial second messenger. *Microbiol. Mol. Biol. Rev.* **77**, 1-52 (2013).  
933
- 934 44 Fath, M., Mahanty, H. & Kolter, R. Characterization of a purF operon mutation which affects colicin  
935 V production. *J. Bacteriol.* **171**, 3158-3161 (1989).  
936
- 937 45 Fath, M. J., Zhang, L. H., Rush, J. & Kolter, R. Purification and characterization of colicin V from  
938 *Escherichia coli* culture supernatants. *Biochemistry* **33**, 6911-6917 (1994).  
939
- 940 46 Soliman, S. S. *et al.* An endophyte constructs fungicide-containing extracellular barriers for its host  
941 plant. *Curr. Biol.* **25**, 2570-2576 (2015).  
942
- 943 47 Reinhold-Hurek, B., Büniger, W., Burbano, C. S., Sabale, M. & Hurek, T. Roots shaping their  
944 microbiome: global hotspots for microbial activity. *Ann. Rev. Phytopathol.* **53**, 403-424 (2015).  
945
- 946 48 Compant, S., Clément, C. & Sessitsch, A. Plant growth-promoting bacteria in the rhizo-and  
947 endosphere of plants: their role, colonization, mechanisms involved and prospects for utilization. *Soil*  
948 *Biol. Biochem.* **42**, 669-678 (2010).  
949

- 950 49 Glaeser, S. P. *et al.* Non-pathogenic *Rhizobium radiobacter* F4 deploys plant beneficial activity  
951 independent of its host *Piriformospora indica*. *ISME J. in press* (2015).  
952
- 953 50 Germaine, K. J., Keogh, E., Ryan, D. & Dowling, D. N. Bacterial endophyte-mediated naphthalene  
954 phytoprotection and phytoremediation. *FEMS Microbiol. Lett.* **296**, 226-234 (2009).  
955
- 956 51 Marasco, R. *et al.* A drought resistance-promoting microbiome is selected by root system under  
957 desert farming. *PLoS ONE* **7**, e48479 (2012).  
958
- 959 52 Dandurand, L., Schotzko, D. & Knudsen, G. Spatial patterns of rhizoplane populations of  
960 *Pseudomonas fluorescens*. *Appl. Environ. Microbiol.* **63**, 3211-3217 (1997).  
961
- 962 53 Foster, R. The ultrastructure of the rhizoplane and rhizosphere. *Ann. Rev. Phytopathol.* **24**, 211-234  
963 (1986).  
964
- 965 54 Fukui, R. *et al.* Spatial colonization patterns and interaction of bacteria on inoculated sugar beet  
966 seed. *Phytopathology* **84**, 1338-1345 (1994).  
967
- 968 55 Rovira, A. A study of the development of the root surface microflora during the initial stages of plant  
969 growth. *J. Appl. Bacteriol.* **19**, 72-79 (1956).  
970
- 971 56 Rovira, A. & Campbell, R. Scanning electron microscopy of microorganisms on the roots of wheat.  
972 *Microb. Ecol.* **1**, 15-23 (1974).  
973
- 974 57 Newman, E. & Bowen, H. Patterns of distribution of bacteria on root surfaces. *Soil Biol. Biochem.* **6**,  
975 205-209 (1974).  
976
- 977 58 Mercado-Blanco, J. & Prieto, P. Bacterial endophytes and root hairs. *Plant Soil* **361**, 301-306 (2012).  
978
- 979 59 Danhorn, T. & Fuqua, C. Biofilm formation by plant-associated bacteria. *Annu. Rev. Microbiol.* **61**,  
980 401-422 (2007).  
981
- 982 60 Lee, R. D.-W. & Cho, H.-T. Auxin, the organizer of the hormonal/environmental signals for root hair  
983 growth. *Front. Plant Sci.* **4**, 448 (2013).  
984
- 985 61 Patten, C. L. & Glick, B. R. Bacterial biosynthesis of indole-3-acetic acid. *Can. J. Microbiol.* **42**,  
986 207-220 (1996).  
987
- 988 62 Oldroyd, G. E. Speak, friend, and enter: signalling systems that promote beneficial symbiotic  
989 associations in plants. *Nat. Rev. Microbiol.* **11**, 252-263 (2013).  
990
- 991 63 Du, X., Li, Y., Zhou, Q. & Xu, Y. Regulation of gene expression in *Pseudomonas aeruginosa* M18  
992 by phenazine-1-carboxylic acid. *Appl. Microbiol. Biotechnol.* **99**, 813-825 (2015).  
993
- 994 64 Srivastava, D. & Waters, C. M. A tangled web: regulatory connections between quorum sensing and  
995 cyclic di-GMP. *J. Bacteriol.* **194**, 4485-4493 (2012).  
996
- 997 65 Flemming, H.-C. & Wingender, J. The biofilm matrix. *Nat. Rev. Microbiol.* **8**, 623-633 (2010).  
998
- 999 66 An, S.Q. *et al.* Novel cyclic di-GMP effectors of the YajQ protein family control bacterial virulence.  
1000 *PLoS Pathog.* **10**, e1004429 (2014).

- 1001  
1002 67 Landini, P., Antoniani, D., Burgess, J. G. & Nijland, R. Molecular mechanisms of compounds  
1003 affecting bacterial biofilm formation and dispersal. *Appl. Microbiol. Biotechnol.* **86**, 813-823 (2010).  
1004  
1005 68 Steinberg, N. & Kolodkin-Gal, I. The matrix reloaded: probing the extracellular matrix synchronizes  
1006 bacterial communities. *J. Bacteriol.* **197**, 2092–2103 (2015).  
1007  
1008 69 Cortes-Barco, A., Hsiang, T. & Goodwin, P. Induced systemic resistance against three foliar diseases  
1009 of *Agrostis stolonifera* by (2R, 3R)-butanediol or an isoparaffin mixture. *Annal. Appl. Biol.* **157**, 179-  
1010 189 (2010).  
1011  
1012 70 Mavrodi, D. V. *et al.* Recent insights into the diversity, frequency and ecological roles of phenazines  
1013 in fluorescent *Pseudomonas* spp. *Environmen. Microbiol.* **15**, 675-686 (2013).  
1014  
1015 71 Gurusiddaiah, S., Weller, D., Sarkar, A. & Cook, R. Characterization of an antibiotic produced by a  
1016 strain of *Pseudomonas fluorescens* inhibitory to *Gaeumannomyces graminis* var. tritici and *Pythium*  
1017 spp. *Antimicrob. Agents Chemotherap.* **29**, 488-495 (1986).  
1018  
1019 72 Anjaiah, V. *et al.* Involvement of phenazines and anthranilate in the antagonism of *Pseudomonas*  
1020 *aeruginosa* PNA1 and Tn5 Derivatives toward *Fusarium* spp. and *Pythium* spp. *Mol. Plant-Microb.*  
1021 *Interact.* **11**, 847-854 (1998).  
1022  
1023 73 Bloemberg, G. V. & Lugtenberg, B. J. Phenazines and their role in biocontrol by *Pseudomonas*  
1024 bacteria. *New Phytol.* **157**, 503-523 (2003).  
1025  
1026 74 Hori, M., Nozaki, S., Nagami, K., Asakura, H. & Umezawa, H. Inhibition of DNA synthesis by  
1027 griseolutein in *Escherichia coli* through a possible interaction at the cell surface. *Biochimica et*  
1028 *Biophysica Acta (BBA)-Nuc. Acids Protein Synth.* **521**, 101-110 (1978).  
1029  
1030 75 Hassan, H. M. & Fridovich, I. Mechanism of the antibiotic action pyocyanine. *J. Bacteriol.* **141**, 156-  
1031 163 (1980).  
1032  
1033 76 Hassett, D. J., Schweizer, H. P. & Ohman, D. E. *Pseudomonas aeruginosa* sodA and sodB mutants  
1034 defective in manganese-and iron-cofactored superoxide dismutase activity demonstrate the  
1035 importance of the iron-cofactored form in aerobic metabolism. *J. Bacteriol.* **177**, 6330-6337 (1995).  
1036  
1037 77 Audenaert, K., Pattery, T., Cornelis, P. & Hofte, M. Induction of systemic resistance to *Botrytis*  
1038 *cinerea* in tomato by *Pseudomonas aeruginosa* 7NSK2: role of salicylic acid, pyochelin, and  
1039 pyocyanin. *Mol. Plant. Microbe Interact.* **15**, 1147-1156 (2002).  
1040  
1041 78 Price-Whelan, A., Dietrich, L. E. & Newman, D. K. Rethinking 'secondary' metabolism:  
1042 physiological roles for phenazine antibiotics. *Nat. Chem. Biol.* **2**, 71-78 (2006).  
1043  
1044 79 Wang, Y. & Newman, D. K. Redox reactions of phenazine antibiotics with ferric (hydr) oxides and  
1045 molecular oxygen. *Environ. Sci. Technol.* **42**, 2380-2386 (2008).  
1046  
1047 80 Hernandez, M. & Newman, D. Extracellular electron transfer. *Cell. Mol. Life Sci.* **58**, 1562-1571  
1048 (2001).  
1049  
1050 81 Fu, Y.-C., Zhang, T. & Bishop, P. Determination of effective oxygen diffusivity in biofilms grown in  
1051 a completely mixed biodrum reactor. *Water Sci. Technol.* **29**, 455-462 (1994).

- 1052  
1053 82 Stewart, P. S. Diffusion in biofilms. *J. Bacteriol.* **185**, 1485-1491 (2003).  
1054  
1055 83 Whitchurch, C. B., Tolker-Nielsen, T., Ragas, P. C. & Mattick, J. S. Extracellular DNA required for  
1056 bacterial biofilm formation. *Science* **295**, 1487-1487 (2002).  
1057  
1058 84 Petersen, F. C., Tao, L. & Scheie, A. A. DNA binding-uptake system: a link between cell-to-cell  
1059 communication and biofilm formation. *J. Bacteriol.* **187**, 4392-4400 (2005).  
1060  
1061 85 Das, T., Sharma, P. K., Busscher, H. J., van der Mei, H. C. & Krom, B. P. Role of extracellular DNA  
1062 in initial bacterial adhesion and surface aggregation. *Appl. Environ. Microbiol.* **76**, 3405-3408  
1063 (2010).  
1064  
1065 86 Das, T., Kutty, S. K., Kumar, N. & Manefield, M. Pyocyanin facilitates extracellular DNA binding to  
1066 *Pseudomonas aeruginosa* influencing cell surface properties and aggregation. *PLoS ONE* **8**, e58299  
1067 (2013).  
1068  
1069 87 Das, T. & Manefield, M. Pyocyanin promotes extracellular DNA release in *Pseudomonas*  
1070 *aeruginosa*. *PLoS ONE* **7**, e46718. (2012).  
1071  
1072 88 Das, T. *et al.* Phenazine virulence factor binding to extracellular DNA is important for *Pseudomonas*  
1073 *aeruginosa* biofilm formation. *Sci. Rep.* **5**, 8398 (2015).  
1074  
1075 89 Pierson III, L. S. & Pierson, E. A. Metabolism and function of phenazines in bacteria: impacts on the  
1076 behavior of bacteria in the environment and biotechnological processes. *Appl. Microbiol. Biotechnol.*  
1077 **86**, 1659-1670 (2010).  
1078  
1079 90 Gérard, F., Pradel, N. & Wu, L.-F. Bactericidal activity of colicin V is mediated by an inner  
1080 membrane protein, SdaC, of *Escherichia coli*. *J. Bacteriol.* **187**, 1945-1950 (2005).  
1081  
1082 91 Gillor, O. & Ghazaryan, L. Recent advances in bacteriocin application as antimicrobials. *Recent Pat.*  
1083 *Anti-infect. Drug Discov.* **2**, 115-122 (2007).  
1084  
1085 92 Hammami, I., Triki, M. & Rebai, A. Purification and characterization of the novel bacteriocin bac  
1086 ih7 with antifungal and antibacterial properties. *J. Plant Pathol.* **93**, 443-454 (2011).  
1087  
1088 93 Dahiya, N., Tewari, R. & Hoondal, G. S. Biotechnological aspects of chitinolytic enzymes: a review.  
1089 *Appl. Microbiol. Biotechnol.* **71**, 773-782 (2005).  
1090  
1091 94 Dahiya, N., Tewari, R., Tiwari, R. P. & Hoondal, G. S. Production of an antifungal chitinase from  
1092 *Enterobacter* sp. NRG4 and its application in protoplast production. *World J. Microbiol. Biotechnol.*  
1093 **21**, 1611-1616 (2005).  
1094  
1095 95 Burkhead, K. D., Slininger, P. J. & Schisler, D. A. Biological control bacterium *Enterobacter*  
1096 *cloacae* S11:T:07 (NRRL B-21050) produces the antifungal compound phenylacetic acid in  
1097 Sabouraud maltose broth culture. *Soil Biol. Biochem.* **30**, 665-667 (1998).  
1098  
1099 96 Slininger, P., Burkhead, K. & Schisler, D. Antifungal and sprout regulatory bioactivities of  
1100 phenylacetic acid, indole-3-acetic acid, and tyrosol isolated from the potato dry rot suppressive  
1101 bacterium *Enterobacter cloacae* S11: T: 07. *J. Ind. Microbiol. Biotechnol.* **31**, 517-524 (2004).  
1102

- 1103 97 Schisler, D. A., Slininger, P. J., Kleinkopf, G., Bothast, R. J. & Ostrowski, R. C. Biological control  
1104 of *Fusarium* dry rot of potato tubers under commercial storage conditions. *Am. J. Potato Res.* **77**, 29-  
1105 40 (2000).  
1106
- 1107 98 Herbert, R. B. & Knaggs, A. R. Biosynthesis of the antibiotic obafluorin from p-aminophenylalanine  
1108 and glycine (glyoxylate). *J. Chem. Soci. (Perkin Transactions)* **1**, 109-113 (1992).  
1109
- 1110 99 Lewis, E. A., Adamek, T. L., Vining, L. C. & White, R. L. Metabolites of a blocked chloramphenicol  
1111 producer. *J. Nat. Prod.* **66**, 62-66 (2003).  
1112
- 1113 100 He, J., Magarvey, N., Pirae, M. & Vining, L. The gene cluster for chloramphenicol biosynthesis in  
1114 *Streptomyces venezuelae* ISP5230 includes novel shikimate pathway homologues and a  
1115 monomodular non-ribosomal peptide synthetase gene. *Microbiology* **147**, 2817-2829 (2001).  
1116
- 1117 101 Wang, K., Kang, L., Anand, A., Lazarovits, G. & Mysore, K. S. Monitoring *in planta* bacterial  
1118 infection at both cellular and whole-plant levels using the green fluorescent protein variant GFPuv.  
1119 *New Phytol.* **174**, 212-223 (2007).  
1120
- 1121 102 Solovyev, V. & Salamov, A. Automatic annotation of microbial genomes and metagenomic  
1122 sequences. in *Metagenomics and its Applications in Agriculture, Biomedicine and Environmental*  
1123 *Studies* (ed. Robert, W. Li), 61-78 (Nova Science, 2011).  
1124
- 1125 103 de Jong, A., Pietersma, H., Cordes, M., Kuipers, O. P. & Kok, J. PePPER: a webserver for prediction  
1126 of prokaryote promoter elements and regulons. *BMC Genom.* **13**, 299 (2012).  
1127
- 1128 104 Stepanović, S., Vuković, D., Dakić, I., Savić, B. & Švabić-Vlahović, M. A modified microtiter-plate  
1129 test for quantification of staphylococcal biofilm formation. *J. Microbiol. Methods* **40**, 175-179  
1130 (2000).  
1131
- 1132 105 Bacon, C., Hinton, D. & Hinton, A. Growth-inhibiting effects of concentrations of fusaric acid on the  
1133 growth of *Bacillus mojavensis* and other biocontrol *Bacillus* species. *J. Appl. Microbiol.* **100**, 185-  
1134 194 (2006).  
1135
- 1136 106 Paulus, H. & Gray, E. The biosynthesis of polymyxin B by growing cultures of *Bacillus polymyxa*. *J.*  
1137 *Biol. Chem.* **239**, 865-871 (1964).  
1138
- 1139 107 Shehata, H. Molecular and physiological mechanisms underlying the antifungal and nutrient  
1140 acquisition activities of beneficial microbes. *PhD thesis, University of Guelph, ON Canada.* (2016).

1141

1142

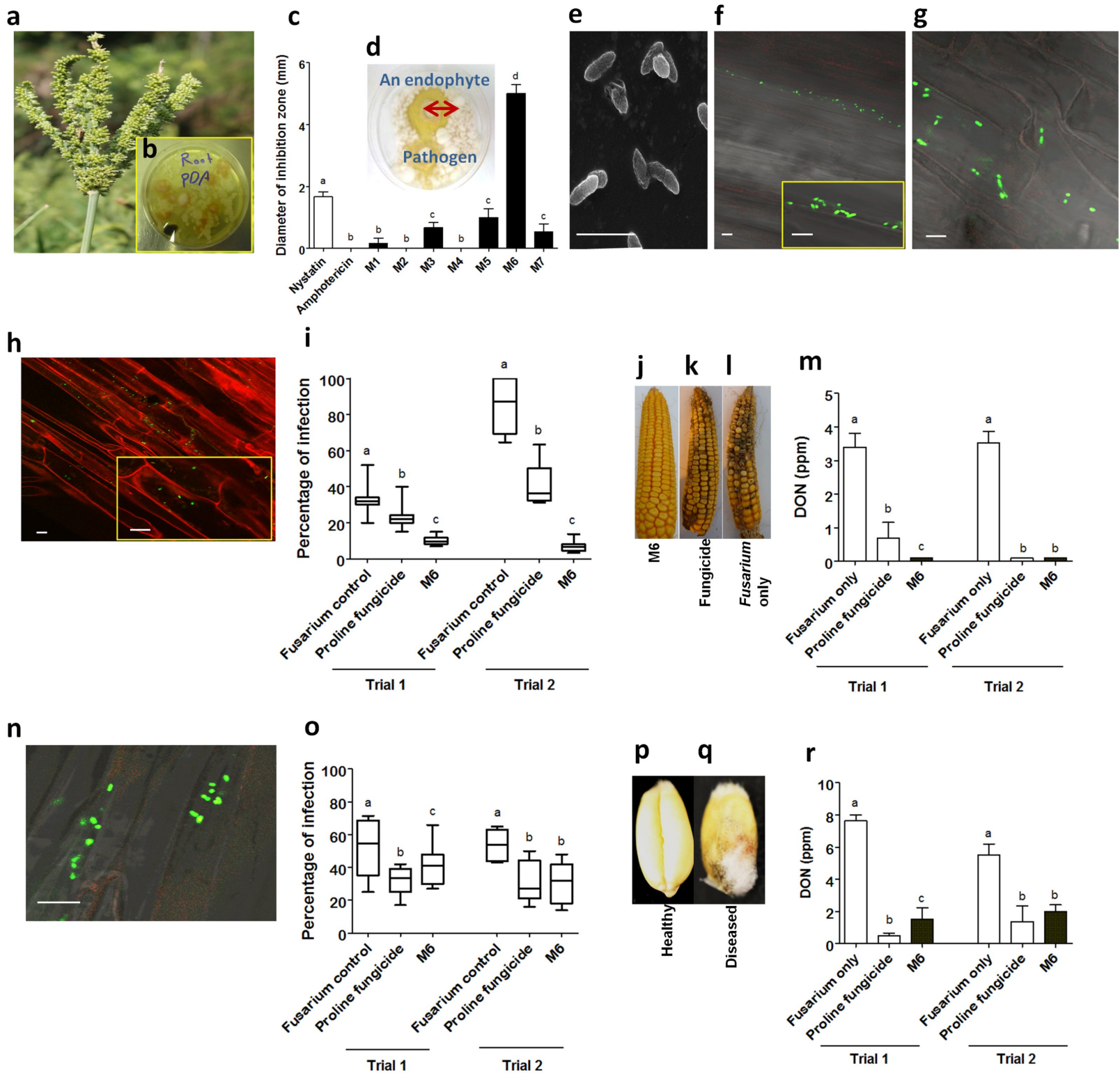
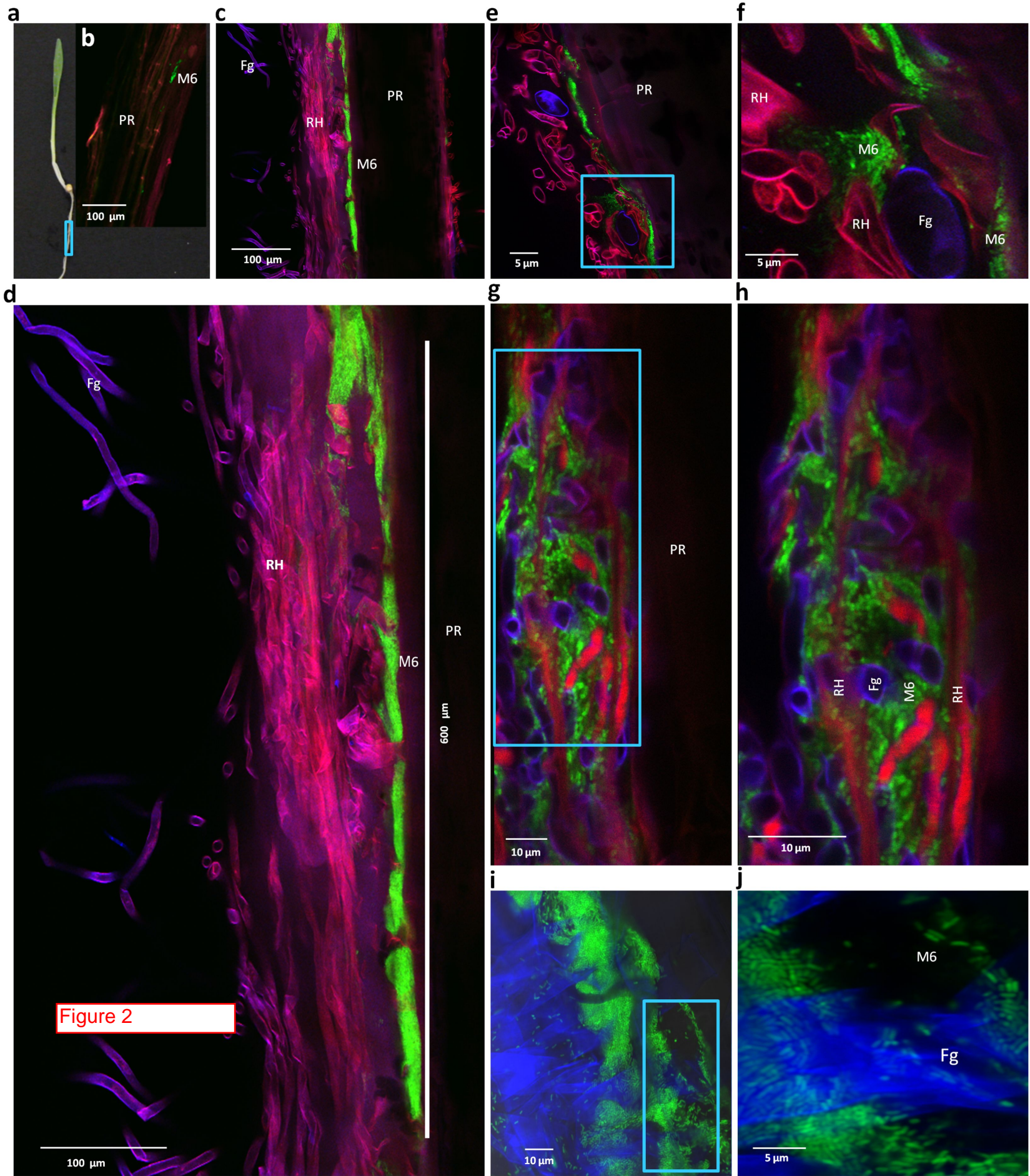


Figure 1



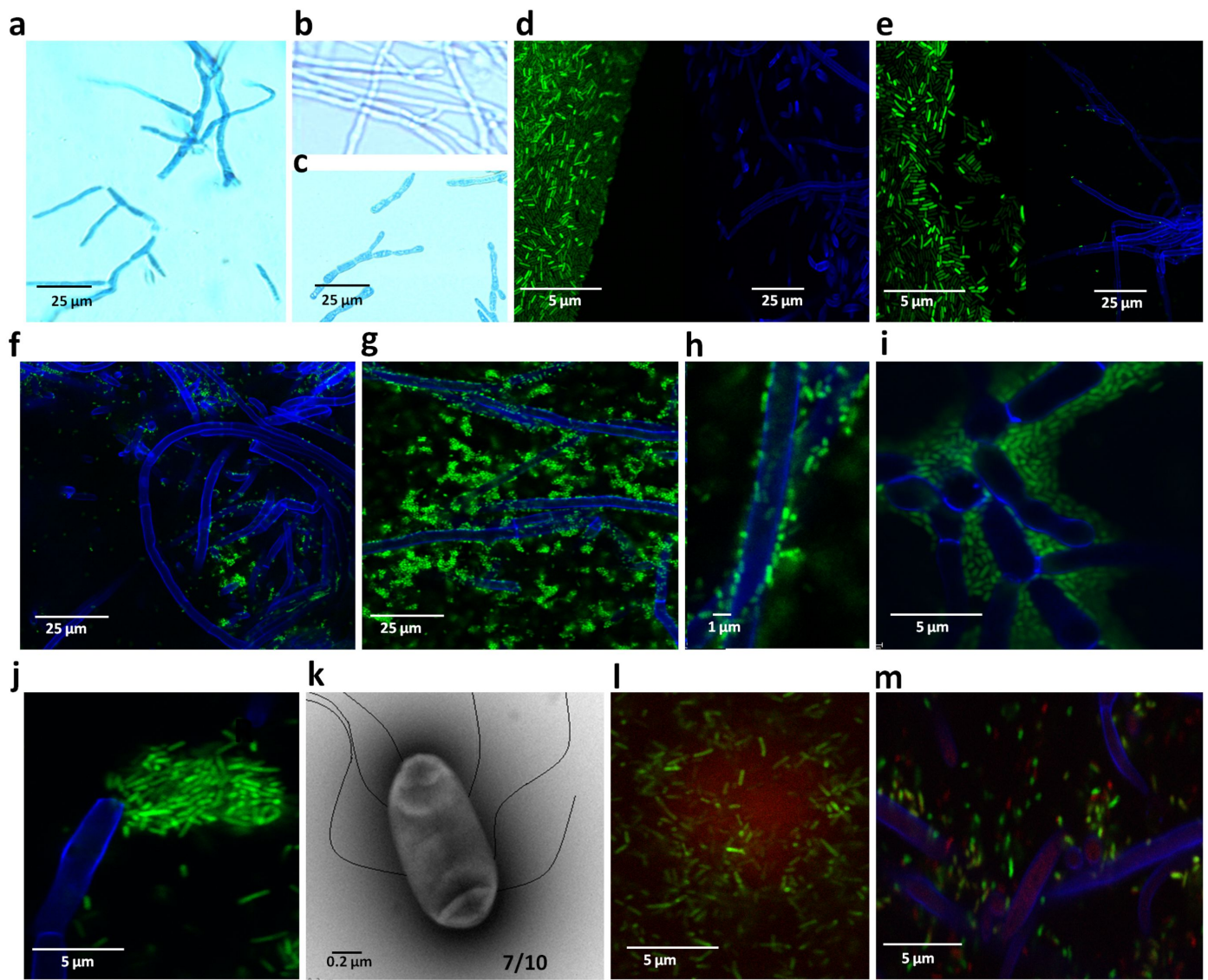


Figure 3

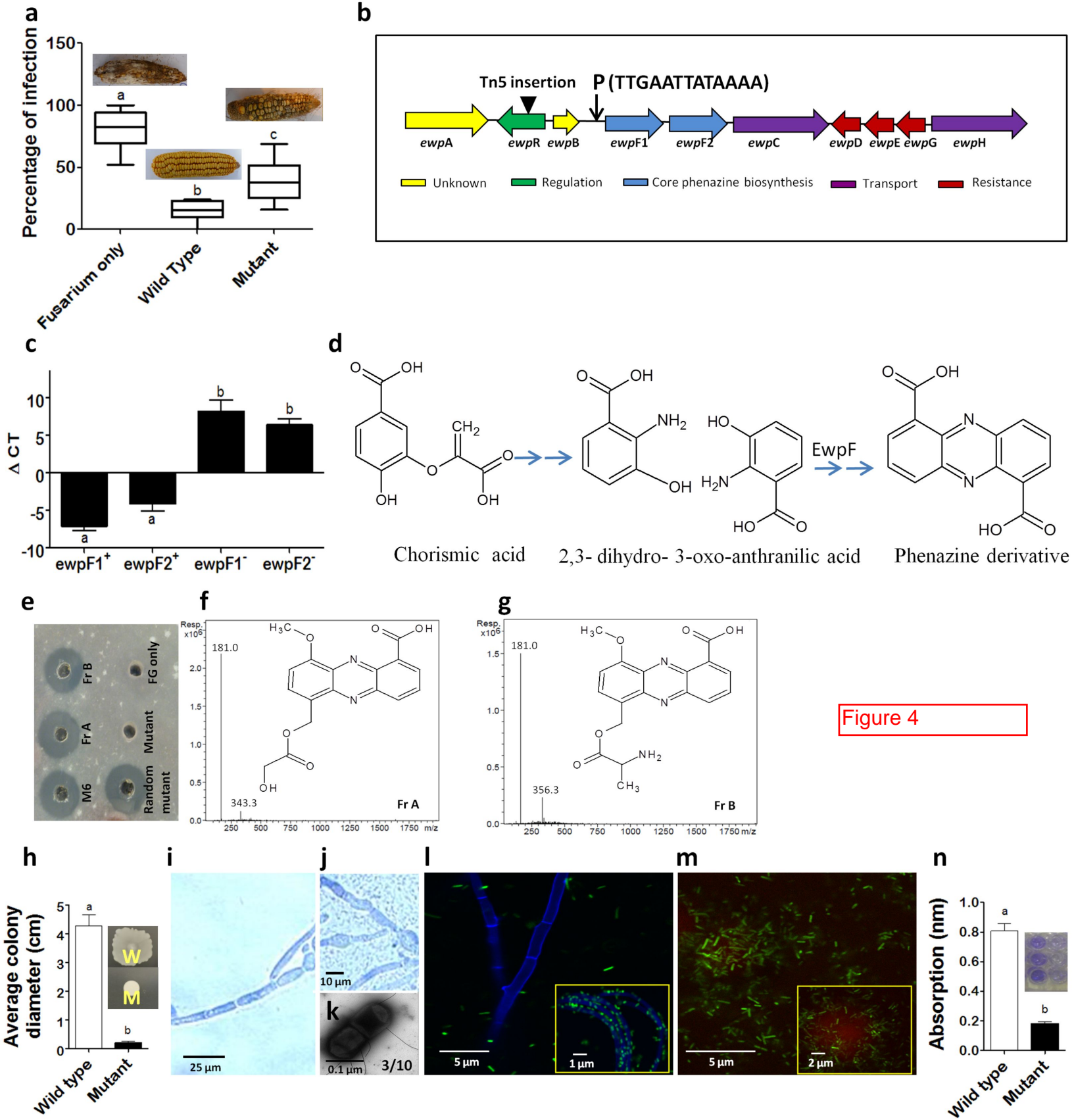
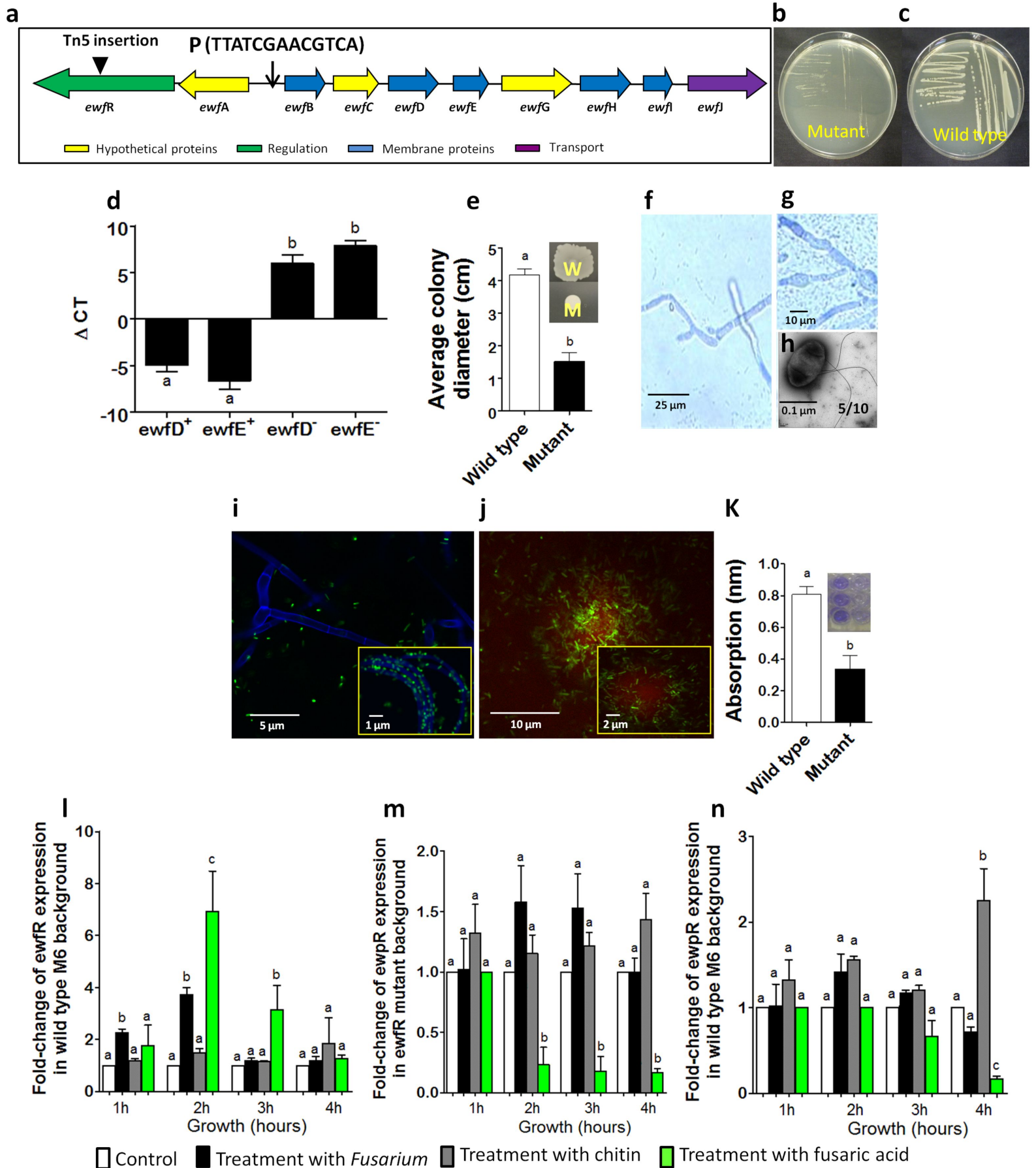


Figure 5



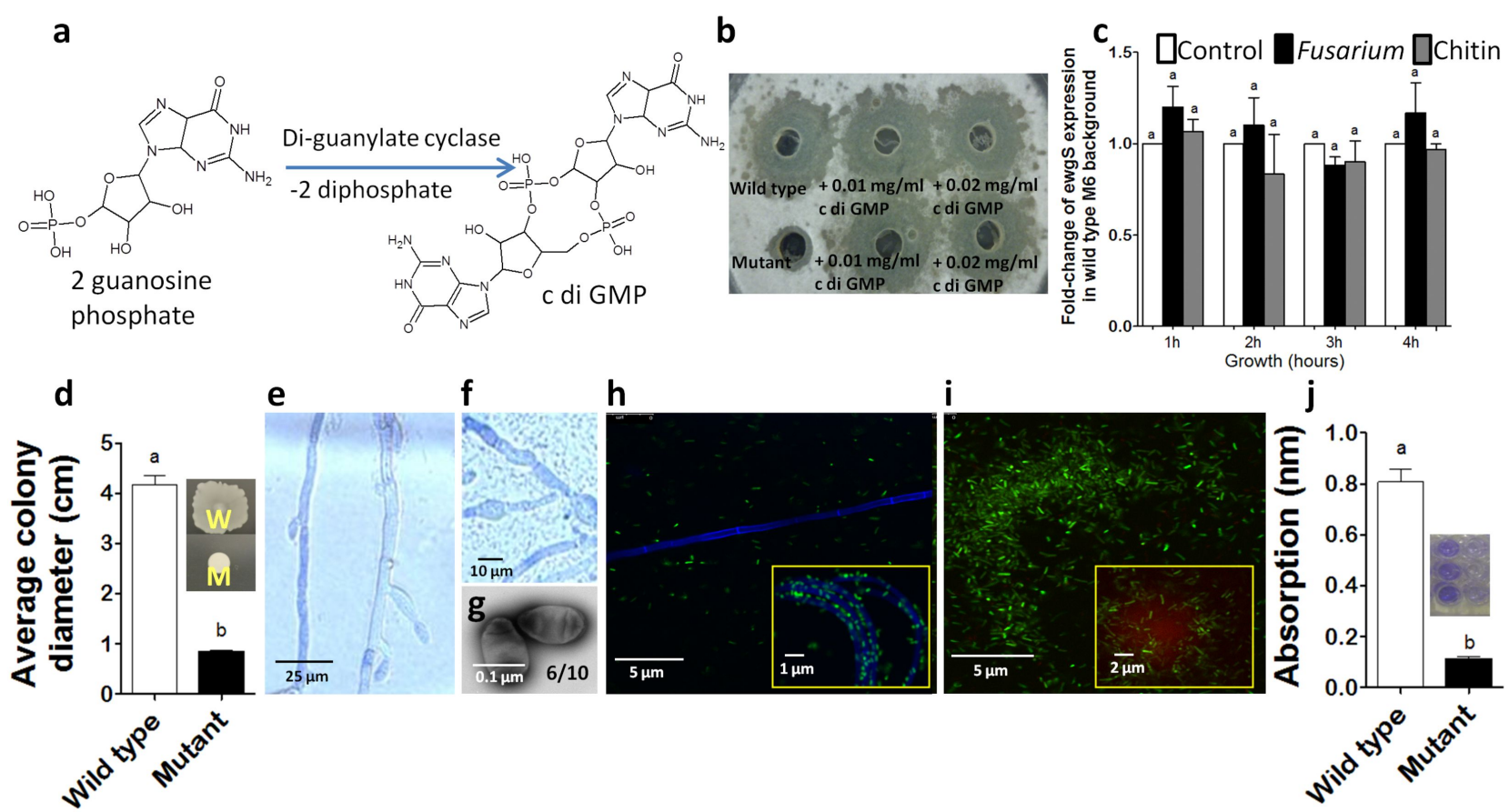


Figure 6

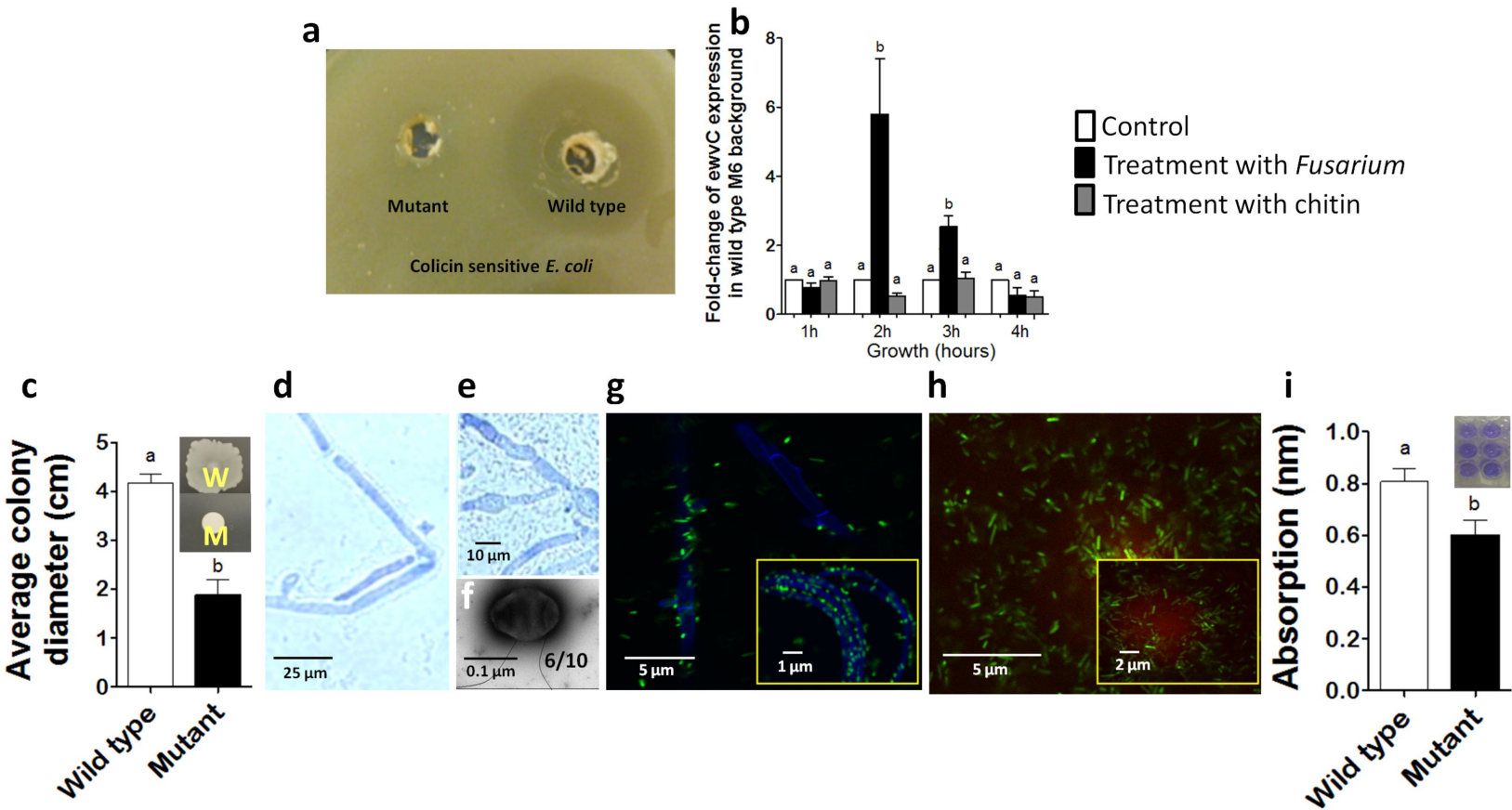


Figure 7

Figure S1

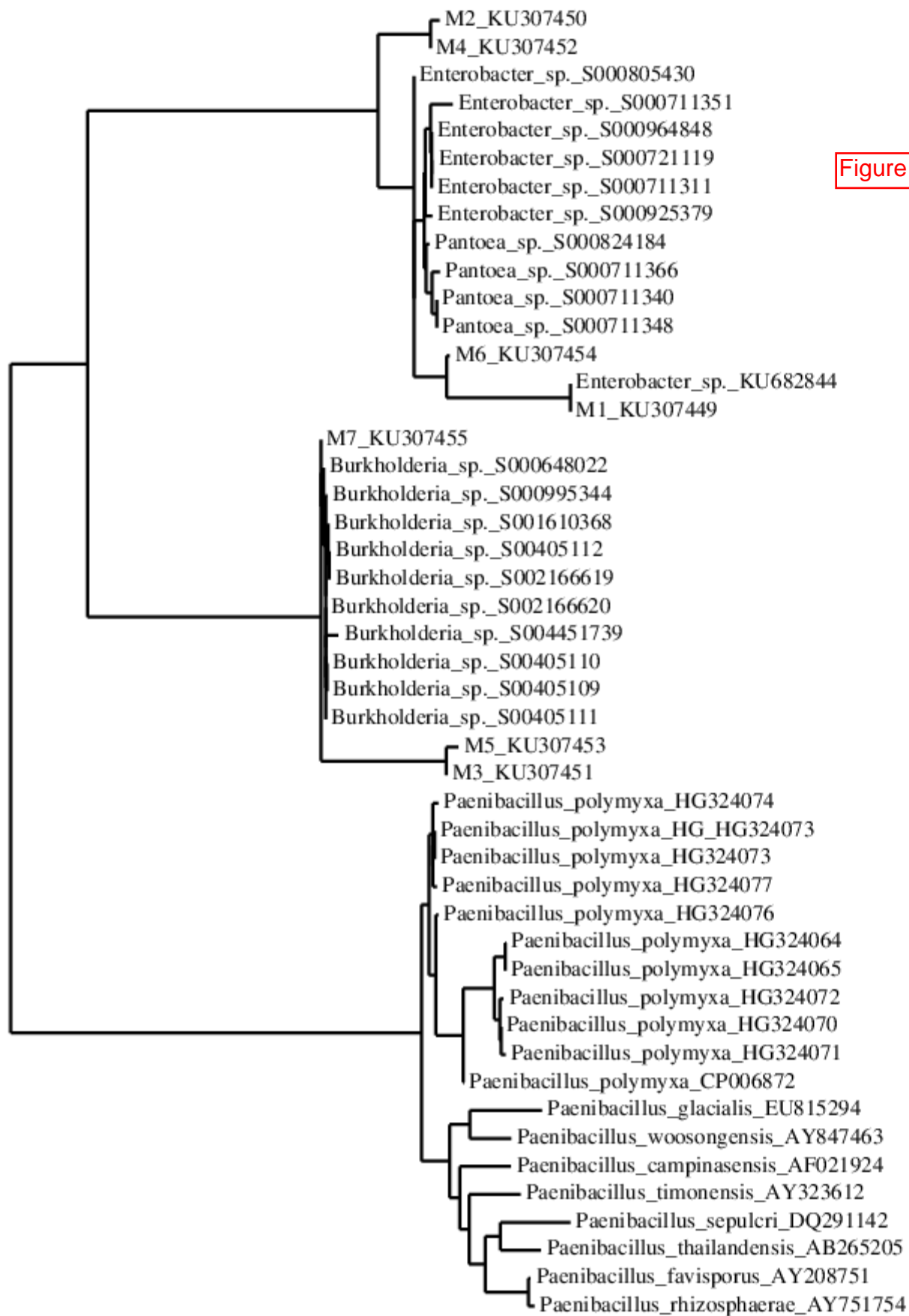


Figure S2



Figure S3

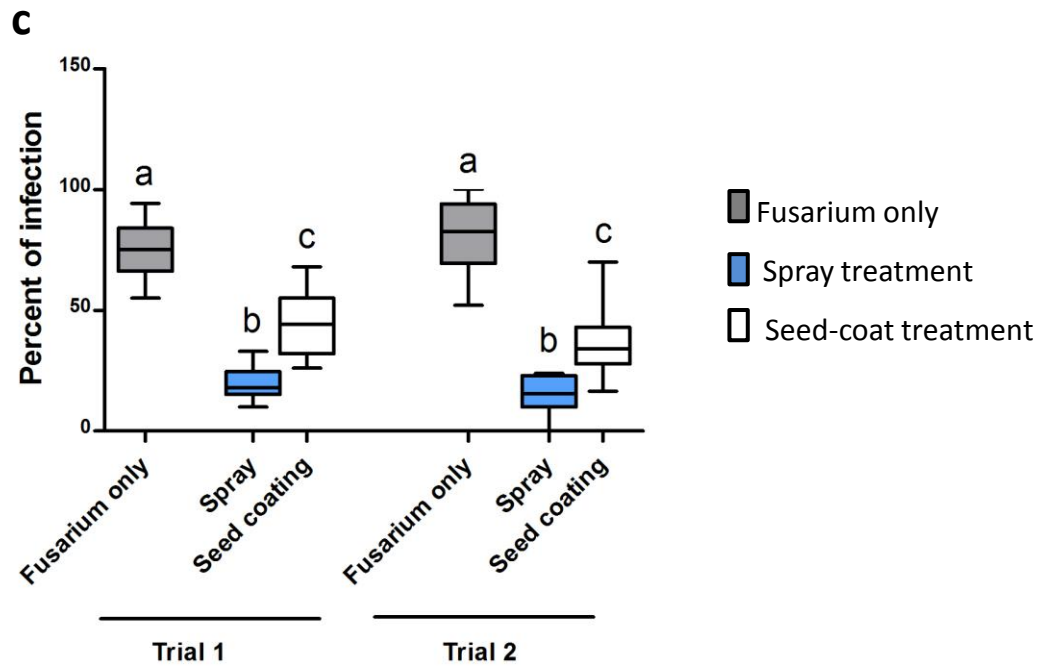
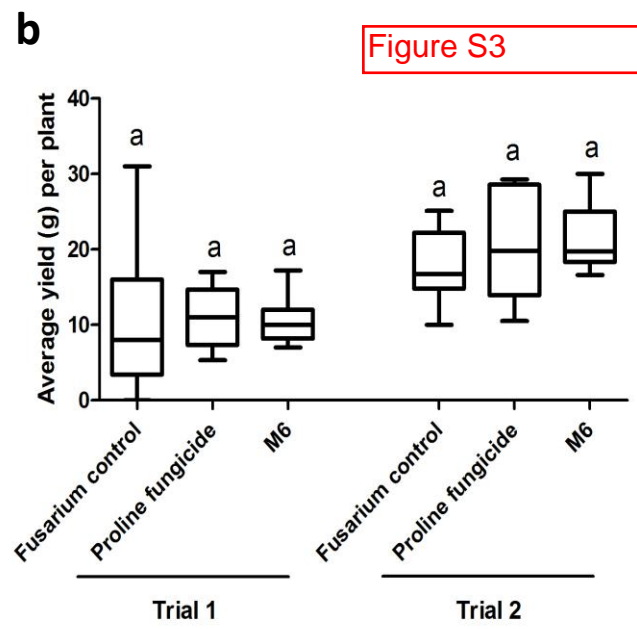
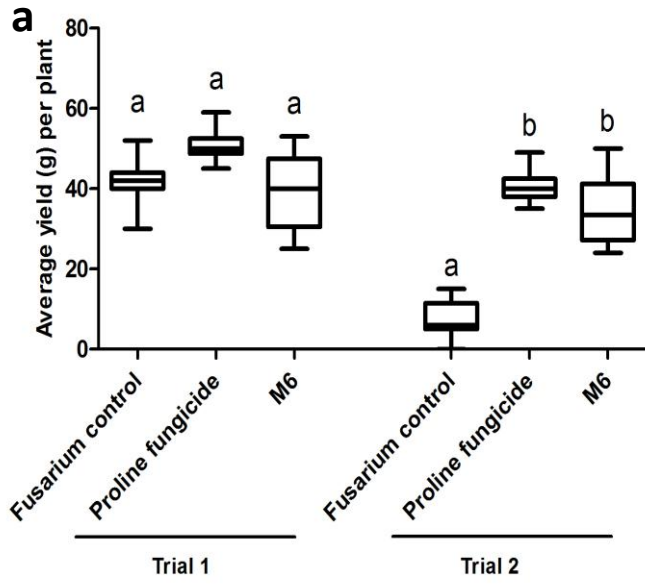
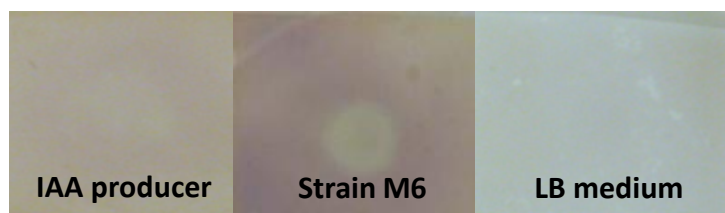


Figure S4



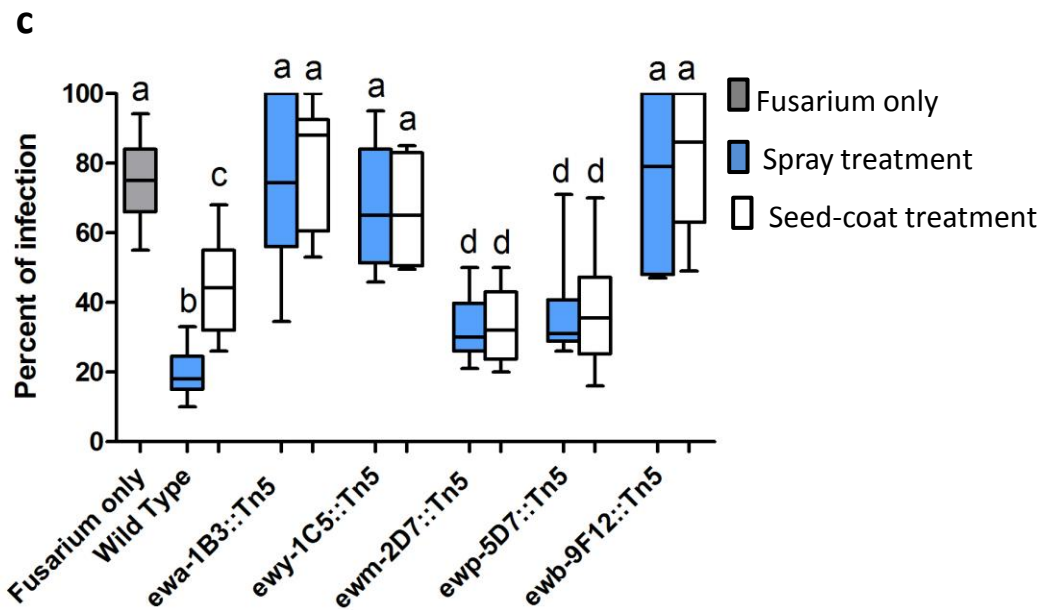
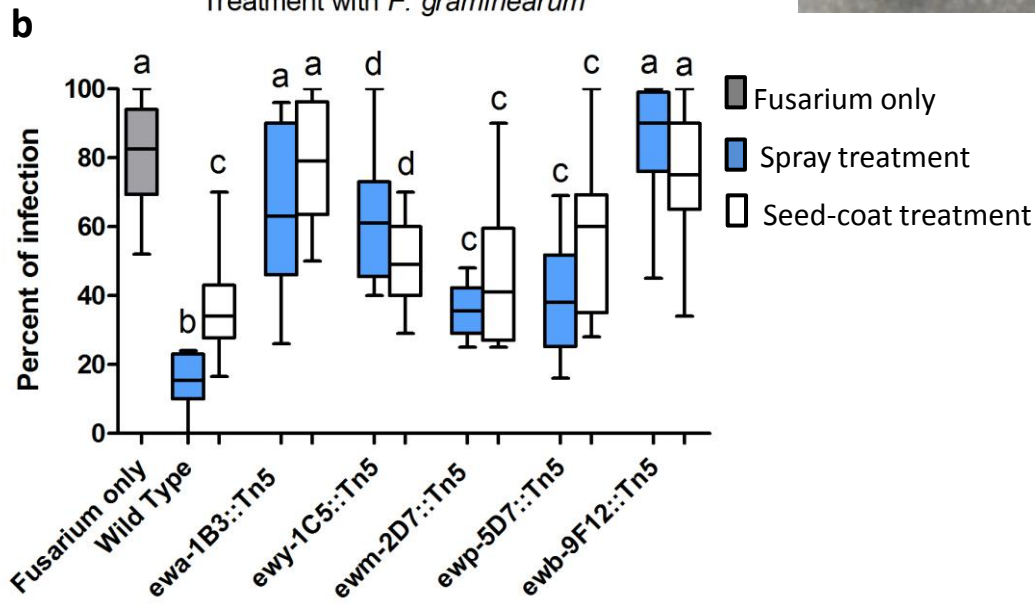
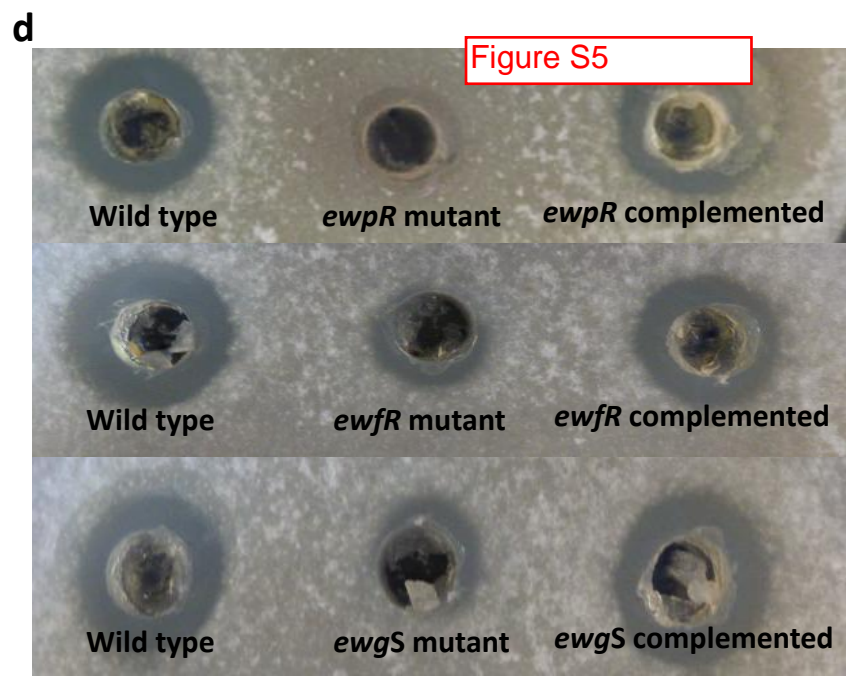
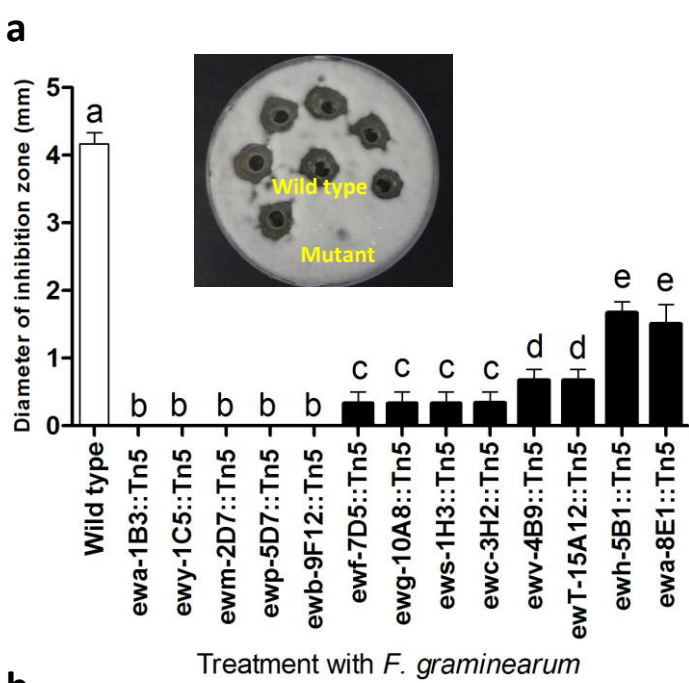


Figure S6

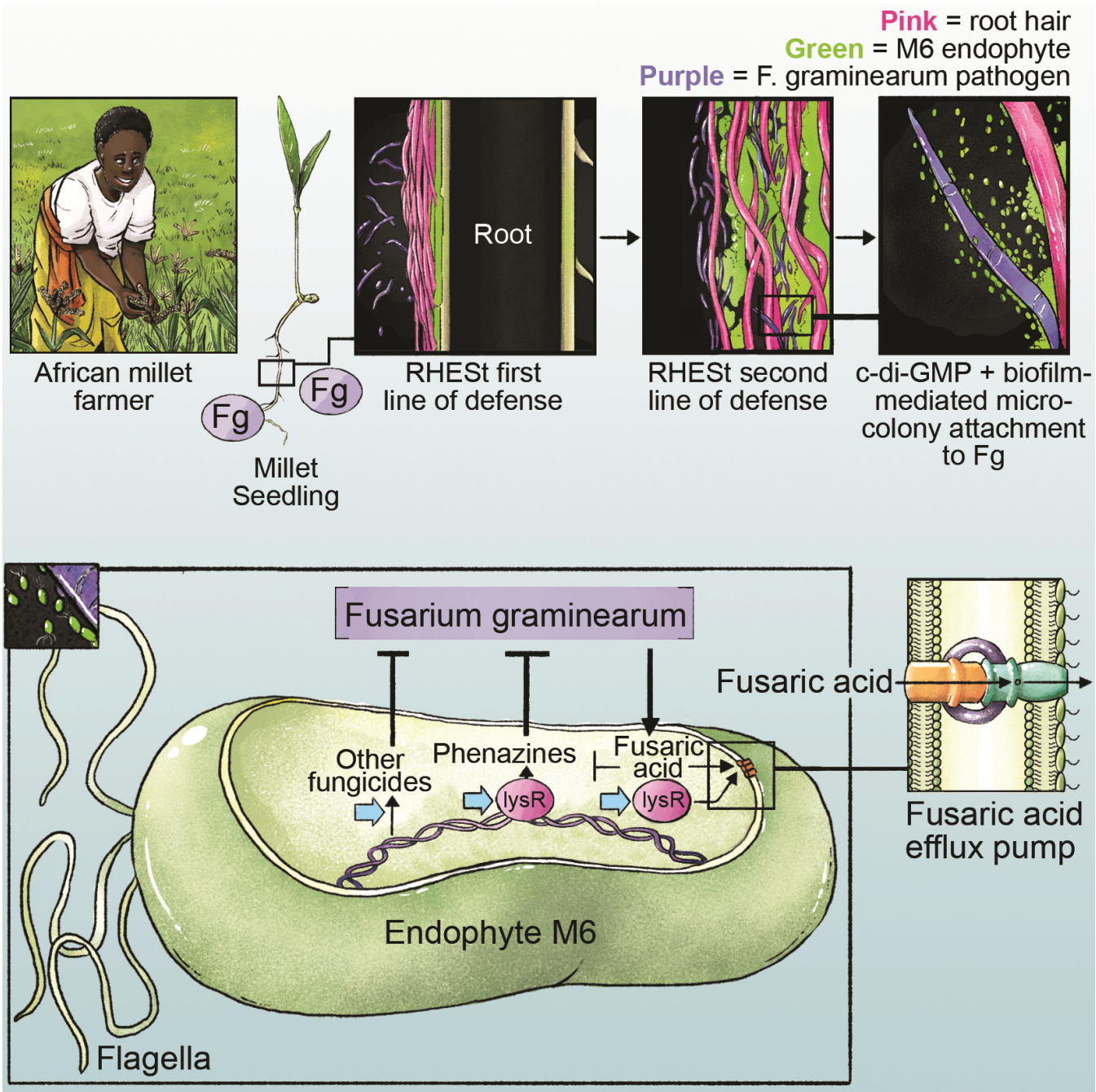
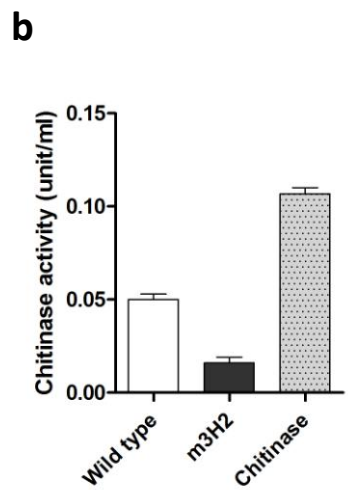
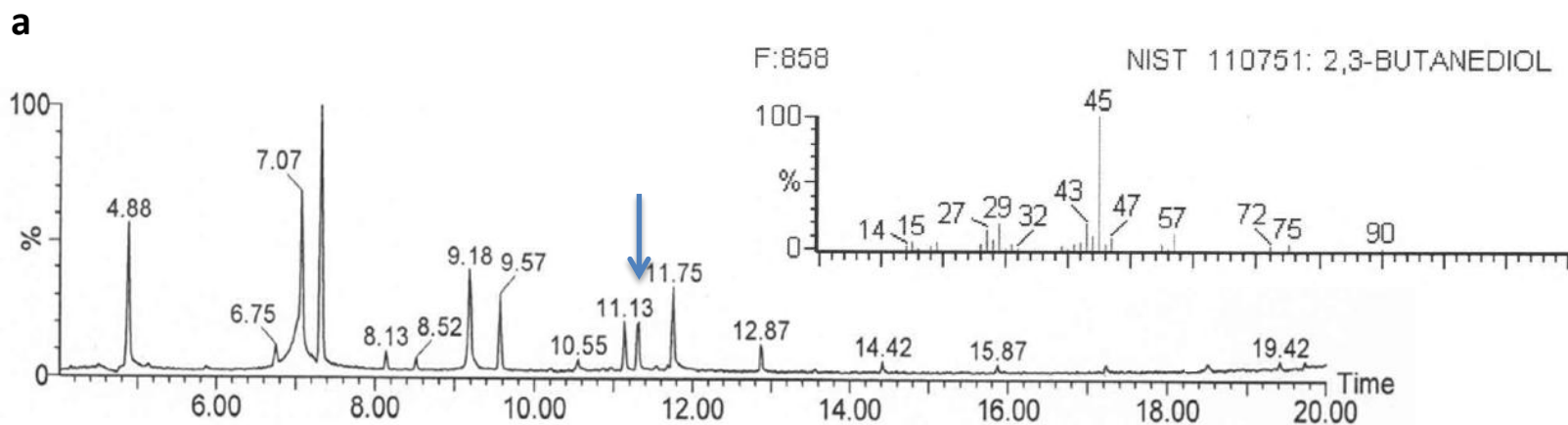


Figure S7



**Supplementary Table 1. Taxonomic classification of finger millet bacterial endophytes based on 16S rDNA sequences and BLAST analysis**

| <b>ID (Genbank Accession)</b> | <b>Tissue source</b> | <b>BLAST analysis</b>              | <b>% of max. identity</b> | <b>Length of aligned sequence</b> |
|-------------------------------|----------------------|------------------------------------|---------------------------|-----------------------------------|
| M1(KU307449)                  | Roots                | <i>Enterobacter</i> sp. (CP015227) | 99                        | 646                               |
| M2 (KU307450)                 | Seeds                | <i>Pantoea</i> sp. (FN796868)      | 99                        | 701                               |
| M3(KU307451)                  | Seeds                | <i>Burkholderia</i> sp. (KC522298) | 99                        | 587                               |
| M4 (KU307452)                 | Shoots               | <i>Pantoea</i> sp. (KT075171)      | 95                        | 751                               |
| M5 (KU307453)                 | Shoots               | <i>Burkholderia</i> sp. (KP455296) | 99                        | 586                               |
| M6 KU307454                   | Roots                | <i>Enterobacter</i> sp. (KU935452) | 99                        | 586                               |
| M7 (KU307455)                 | Shoots               | <i>Burkholderia</i> sp. (HQ023278) | 100                       | 644                               |

**Supplementary Table 2. Effect of endophyte strain M6 isolated from finger millet on the growth of diverse fungal pathogens *in vitro*.**

| Target fungal species                 | Diameter of growth inhibition zone in mm |                             |          |
|---------------------------------------|--|-----------------------------|----------|
|                                       | Nystatin<br>(10.0 U/ml)                  | Amphotericin<br>(250 µg/ml) | M6       |
| <i>Alternaria alternata</i>           | 0.0±0.0                                  | 0.0±0.0                     | 0.0±0.0  |
| <i>Alternaria arborescens</i>         | 0.0±0.0                                  | 0.0±0.0                     | 0.0±0.0  |
| <i>Aspergillus flavus</i>             | 2.0±0.2                                  | 0.0±0.0                     | 3.6±0.2  |
| <i>Aspergillus niger</i>              | 0.0±0.0                                  | 2.0±0.0                     | 0.0±0.0  |
| <i>Bionectria ochroleuca</i>          | 2.0±0.2                                  | 0.5±0.2                     | 0.0±0.0  |
| <i>Davidiella tassiana</i>            | 1.5±0.2                                  | 0.5±0.3                     | 0.0±0.0  |
| <i>Diplodia pinea</i>                 | 2.5±0.2                                  | 3.0±0.2                     | 0.0±0.0  |
| <i>Diplodia seriata</i>               | 3.0±0.2                                  | 2.0±0.2                     | 0.0±0.0  |
| <i>Epicoccum nigrum</i>               | 0.0±0.0                                  | 0.0±0.0                     | 0.0±0.0  |
| <i>Fusarium avenaceum</i> (isolate 1) | 2.5±0.3                                  | 3.0±0.6                     | 1.8±0.2  |
| <i>Fusarium graminearum</i>           | 1.5±1.6                                  | 0.0±0.0                     | 5.0±0.3  |
| <i>Fusarium lateritium</i>            | 0.0±0.0                                  | 1.0±0.2                     | 0.0±0.0  |
| <i>Fusarium sporotrichioides</i>      | 1.0±0.2                                  | 1.0±0.2                     | 2.8±0.2  |
| <i>Fusarium avenaceum</i> (isolate 2) | 0.0±0.0                                  | 0.0±0.0                     | 0.0±0.0  |
| <i>Nigrospora oryzae</i>              | 0.0±0.0                                  | 0.0±0.0                     | 1.83±0.2 |
| <i>Nigrospora sphaerica</i>           | 0.0±0.0                                  | 0.0±0.0                     | 0.0±0.0  |
| <i>Paraconiothyrium brasiliense</i>   | 0.0±0.0                                  | 0.0±0.0                     | 0.0±0.0  |
| <i>Penicillium afellutanum</i>        | 3.0±0.2                                  | 3.0±0.2                     | 0.0±0.0  |
| <i>Penicillium expansum</i>           | 2.0±0.2                                  | 5.0±0.2                     | 4.9±0.1  |
| <i>Penicillium olsonii</i>            | 1.5±0.3                                  | 3.5±0.3                     | 0.0±0.0  |
| <i>Rosellinia corticium</i>           | 2.0±0.2                                  | 4.5±0.3                     | 0.0±0.0  |

**Supplementary Table 3. Suppression of *F. graminearum* disease symptoms in maize and wheat by endophyte M6 in replicated greenhouse trials.**

| <b>Treatment</b>                   | <b>% Infection (mean ± SEM)*</b> | <b>% Disease reduction relative to <i>Fusarium</i> only treatment</b> | <b>Average yield per plant*</b> | <b>% Yield increase relative to <i>Fusarium</i> only treatment</b> |
|------------------------------------|----------------------------------|---|---------------------------------|--|
| <b>Greenhouse trial 1 in maize</b> |                                  |   |                                 |  |
| <i>Fusarium</i> only               | 33.69±2.3                        | 0.0   | 41.77±1.4                       | 0.0  |
| Proline fungicide                  | 23.10±2.0                        | 31.4  | 50.9±1.2                        | 21.85  |
| M6                                 | 10.13±0.9                        | 69.93   | 39.58±2.6                       | -5.2   |
| <b>Greenhouse trial 2 in maize</b> |                                  |   |                                 |  |
| <i>Fusarium</i> only               | 85.11±4.5                        | 0.0   | 7.8±1.1                         | 0.0  |
| Proline fungicide                  | 41.42±4.5                        | 51.33   | 40.8±1.2                        | 423  |
| M6                                 | 6.9±0.9                          | 91.89   | 34.70±2.7                       | 344  |
| <b>Greenhouse trial 1 in wheat</b> |                                  |   |                                 |  |
| <i>Fusarium</i> only               | 51.8±6.3                         | 0.0   | 10.5±2.6                        | 0.0  |
| Proline fungicide                  | 31.70±2.6                        | 38.8  | 10.9±1.3                        | 3.8  |
| M6                                 | 41.1±2.6                         | 20.6  | 10.6±0.8                        | 0.95   |
| <b>Greenhouse trial 2 in wheat</b> |                                  |   |                                 |  |
| <i>Fusarium</i> only               | 54.0±2.6                         | 0.0   | 17.7±1.5                        | 0.0  |
| Proline fungicide                  | 31.5±4.1                         | 41.6  | 20.1±2.1                        | 13.5   |
| M6                                 | 30.7±3.6                         | 43.1  | 21.1±1.3                        | 19.2%  |

\*SEM is the standard error of the mean.

**Supplementary Table 4. Reduction of DON mycotoxin accumulation during prolonged seed storage following treatment with endophyte M6.**

| <b>Treatment</b>                    | <b>DON content (ppm)<br/>(mean ± SEM)*</b> | <b>% DON reduction relative to<br/>Fusarium only treatment*</b> |
|-------------------------------------|--|---|
| <b>Greenhouse trial 1 in maize</b>  |  |   |
| <i>Fusarium</i> only                | 3.4±0.4                                    | 0.0   |
| Proline fungicide                   | 0.7±0.4                                    | 79.4  |
| M6                                  | 0.1±0.0                                    | 97  |
| <b>Greenhouse trial 2 in maize</b>  |  |   |
| <i>Fusarium</i> only                | 3.5±0.3                                    | 0.0   |
| Proline fungicide                   | 0.1±0.0                                    | 97.1  |
| M6                                  | 0.1±0.0                                    | 97.1  |
| <b>Green house trial 1 in wheat</b> |  |   |
| <i>Fusarium</i> only                | 7.6±0.3                                    | 0.0   |
| Proline fungicide                   | 0.5±0.1                                    | 94.6  |
| M6                                  | 1.5±0.6                                    | 81.33   |
| <b>Green house trial 2 in wheat</b> |  |   |
| <i>Fusarium</i> only                | 5.5±0.7                                    | 0.0   |
| Proline fungicide                   | 1.3±0.9                                    | 76.3  |
| M6                                  | 2.0±0.4                                    | 63.6  |

**\*SEM is the standard error of the mean.**

**Supplementary Table 5. Complete list of strain M6 Tn5 insertion mutants showing loss of antifungal activity against *F. graminearum* in vitro.**

| ID  | Gene prediction  | Swarming assay | Motility assay (mean ± SEM)* | Presence of flagella (%) | Biofilm (mean ± SEM)* |
|---|--|----------------|------------------------------|--------------------------|-----------------------|
| Wild type                                   |  | +++            | 4.2±0.3                      | 70%                      | 0.8                   |
| <i>ewa-1B3::Tn5</i><br><i>ewa-4B8::Tn5</i>  | Transcription regulator, AraC  | ---            | 0.6±0.02                     | 50%                      | 0.11±0.00             |
| <i>ewy-1C5::Tn5</i><br><i>ewy-5D2::Tn5</i>  | YjbH outer-membrane protein  | ++             | 0.5±0.03                     | 10%                      | 0.3±0.08              |
| <i>ewm-2D7::Tn5</i>                         | 4-hydroxyphenyl acetate 3-monoxygenase<br><br>May catalyze production of phenylacetic acid (PAA)               | ---            | 0.8±0.05                     | 20%                      | 0.07±0.00             |
| <i>ewpR-5D7::Tn5</i>                        | Transcription regulator, LysR  | ---            | 0.5±0.03                     | 30%                      | 0.18±0.01             |
| <i>ewb-9F12::Tn5</i><br><i>ewb-7C5::Tn5</i> | Fatty acid biosynthesis  | ---            | 0.6±0.05                     | 30%                      | 0.3±0.11              |
| <i>ewvC-4B9::Tn5</i>                        | Colicin V production   | +              | 1.8±0.30                     | 60%                      | 0.6±0.05              |
| <i>ewT-15A12::Tn5</i>                       | Transport permease protein<br><br>Within operon for biosynthesis of P-amino-phenyl-alanine antibiotics (PAPA). | +              | 1.5±0.00                     | 30%                      | 0.6±0.04              |
| <i>ews-1H3::Tn5</i>                         | Sensor histidine kinase  | +              | 0.8±0.16                     | 50%                      | 0.8±0.2               |
| <i>ewc-3H2::Tn5</i>                         | Chitinase  | ---            | 1.0±0.00                     | 20%                      | 0.4±0.15              |
| <i>ewfR-7D5::Tn5</i>                        | Transcription regulator, LysR  | +              | 1.5±0.20                     | 50%                      | 0.3±0.08              |
| <i>ewgS-10A8::Tn5</i>                       | Di-guanylate cyclase   | ---            | 0.8±0.30                     | 40%                      | 0.1±0.01              |
| <i>ewh-5B1::Tn5</i>                         | Hig A protein  | +++            | 1.6±0.30                     | 30%                      | 0.6±0.10              |
| <i>ewa-8E1::Tn5</i>                         | Hypothetical protein   | ++             | 2.3±0.40                     | 20%                      | 0.5±0.09              |

\*SEM is the standard error of the mean.

**Supplementary Table 6. M6 wild type nucleotide coding sequences (Ettinger et al, 2015) corresponding to Tn5 insertion mutants that showed loss of antifungal activity against *F. graminearum* in vitro**

| ID                  | Gene sequence  |
|---------------------|--|
| <i>ewa-1B3::Tn5</i> | <p>gtgaataccattggcataaacagcgagcccatcctgacgcacagtggcttagcattaccgccgatacc<br/> actcttgccgcagacaggcaactatgacgttatctatctctcctgccctgtggcgaatcctcgtgacgtggc<br/> agacaacagcctgaactcctggcatggcttagcgaacaggcggcgcgaggaccgccatcgcggcc<br/> gtcggaaacgggctgctgtttcctggcgaatcgggattgctcaacgggaaaccgccaccaccactg<br/> gcactactcaaacagttctcgcgtgactacccaacgtaaaattacaaccaaaccattttctacgcag<br/> gccgataatatttactgtgcccagcgtcaaagccctctcagatctgacctccatttcacgaaacgat<br/> atacgggaaacgtgtagccacacatacccaacggaccttttccatgaaattcggagtcagttgatcgc<br/> cagtgttacagtgaagaaaacaaaccatccggatgaagataattgtcaaatcaaatctggataaaa<br/> gccaactcgcctcggatataatccatgaaaatcttgcgatatggctggcatgagtttgcgaactttaa<br/> cgccgtttaaaaatgccaccgatataatccccctgcagatattataaccgccagaattgaatccgcat<br/> gacaatgtgcaatcccaatctgagcattcaggagattgcaatcgggtgggatcaggatattgc<br/> gcacttaatcggcagtttaagcataaaacaacggtttcaccgggggattaccgtaagaccgtccgggc<br/> aaagatgttagtgataa</p>   |
| <i>ewy-1C5::Tn5</i> | <p>atgaaaagaacctatctctacagcatgctggcgtctgctgagtgccgcgtgccatgcagaaacgat<br/> ccggcaccattggcccgtctcagtcagacttcggcggcgtcggtttgctgcaaacgccaccgcgcgg<br/> atggcgcgcgaaggggaaattagccttaactaccgtgataacgatcagatcgttactactcggcgtcgg<br/> tgcagctgttcccgtggctgaaaccacgctgctgctacaccgacgtgctgacgaaacagtaacagcgc<br/> gttgatgcttcccggcgaccagacctacaagataaagccttcgacgtcaagctgcgcctgtgggaa<br/> gagagctactggatgccgacggtgtccgtggggcgcaagatacgggtgaccggctgtttgatgctg<br/> aatacatcgtggccagtaaaagcctgggggcccgttcgacttctcgtcgcctgggatggggctacctgg<br/> gcactggcggtaacgtgaaaaatccgttttgcctcagcgcgataaatactgctaccgcgataacagcta<br/> taagaaagcgggtccatcaacggtagaccagatgttccacggcggcatcgtgtttggcggcgtgga<br/> gtatcaaacgccctggcagccattacgcctgaagctggaatatgaagggaatgactactcgcaggactt<br/> cgccgggaagattgagcagaagagcaagttaacgtcggcggccattatcgcgtcaccgactgggccc<br/> acgttaacctcagctacgagcgcggcaacaccgctgattttggctcagcgtcgcaccaactttaacga<br/> tatcggccacactacaatgataacgcgcgccctgcataaccagccggagccgcaggatgcgattctgc<br/> agcactccgtgtggcaaacagctgacgtgctgaaatacaatccggcctggcggatccgaaaatt<br/> caggtgaaagcgatacgtgtacgtgaccggcagcaggtgaaataaccgcgactcgcgcgaaggg<br/> atcgaacgcgctaaccggatcgtaatgaacgatctgcccggaggggattccgcacgatccgcgtgacgg<br/> aaaaccgccttaacctgcccaggtgacgacggaaacggacgttgccagcctaagcgccatctgga<br/> aggtgaaccgctcggcatgaaaccgagctgggtcaaaaacgcgtgaaaccgatcgtgcccggagac<br/> caccgagcagggctgtatatacgacaaatcgcgcttcgatttccatcagatccggctgtaaccagctcc<br/> gtcggcgggcccggaaaacttctacatgatcagctggcgtcatggcgacggcggatctgtggcttacc<br/> gaccacctgctgaccaccggtagcctgttcggcaacatcgtaataactacgacaagttcaactacacc<br/> aaccgcgcaaaagactcacagctcgcgcgtgctgactcgcgtgctgtaatacgtgcagaacgatg<br/> ctacgtgaaataacctgcaggccaactattccagctactcggcaatggcttctacggccagggtgacggc<br/> gggtatctggaaccatgtacggcggcggggcggaagtgctttatcgtcctgtcagcagcaactgg<br/> gcgttcggggtgatgcaactacgtcaagcagcgtgactggcgcagcgcgaggacatgatgaagtt<br/> caccgactacagcgtcaaacgggcatctgaccgcctactggacgccctcgttcgcgcctgacgtgct<br/> ggtgaaagccagcgttggctcagctacctggcggcgataagggcggtagcgtggatctctaaacactt<br/> cgacagcggcgtcgtgtggcggcgtatgccaccatcaccacgittcgcggacgaatacggggaa<br/> ggggacttcaccaaggggtctacgtgctgattccgctggatctgtctcgtcaggcccaaccgcagcc<br/> gtcggcagtaggctggacggcgtgacgcgtgacgggggtcaacagcttgacgtaagttccagctg<br/> tatgacatgacgagcgataagaacattaactccgctga</p> |

|                      |  |
|----------------------|--|
| <i>ewm-2D7::Tn5</i>  | atgaagcctgaagagttccgctgatgccaacgcccgttaaccggcgaagagtatttaaaagcct<br>gcaggacggctgagatttatctacggcgagcgcgtcaaagacgtcaccacccatccggcatttcg<br>caacggggcggcctccatcgcgcagatgtacgacgcgtgcacaagcctgacatgcaggacgcgctc<br>tgctggggcaccgacaccggcagcggcggtatacccacaagttttccgctggcgaaaagtccga<br>cgacctgcccagcagcgcgacccatcgccgagtggtcgcgctgagctacggctggatggggccg<br>acggcggactaaaagccggttcggctgctgcgctcggcgcaaccggccttctacggccagttcga<br>acagaacgcccgtactggtacacgcgcattcaggaaccggcctgtactttaaccagccatcgtaa<br>cccggcgtcaccgtcacaagccggcgagcgggtgaaagacgtctacatcaagctggagaaag<br>agaccgacgcccggattatcgtcagcggcgcaagtggtagccaccaactccgacctgaccacta<br>caacatgatcggctcggctcgcgaggtgatggcgaaaaccggactcgcgctgatgtcgtcgc<br>gccgatggatgccgaaggcgtgaagctgatctcccgcctcttacgaaatgggtgagggcgaaccg<br>gatccccgtacgactaccgctcaccagccgtttgatgagaacgacgcgatcctggtgatggatcacgt<br>gctgatcccgtgggaaaatgtgctgatctaccgcatcttcgaccgctgcccgtcgtggacgatggaagg<br>cggtttcgcgggatgtaaccgctgacggcctcgtcgtcgtggcggtgaagctcgcactcatcaccgcc<br>ctgtgaagaaatcccggagtgaccggcaccctggagttccgcggtacaggcggatctcggcga<br>agtgggtggcctggcgaacatgttctggcgctgagcgcactcatgttccgaagccaccccgtgggtc<br>aacggcgcgtatcgcggatcacgcgcgctgcaaacctaccgctgatggcgccgatggcctacgc<br>caagatcaagaacatcatcagcgtaacgtgacgtccgctgatctacctgcccagcggccggg<br>atctgaacaaccgcagatcgaccgatctggcgaatacgtgcgcggtccaacgggatggatcac<br>gtcgaacgcataagatttgaagctgatgtgggatccatcggcagcagatttggcggtcgtcagagc<br>tatacgaatacaactactccggcagccaggtgatgagatccgctcagtgctcgcaggcgcagagc<br>tccggcaacatggacaaaatgatggcgtggtcgcaccgctgcatgtccgaatcagaccagcagcgt<br>ggaccgtaccgcacctgcacaacaacagcgatatcaacatgctcgcacaagctgctgaaatag |
| <i>ewp-5D7::Tn5</i>  | atggactaaccagctgaaatgtttaacgcccgtcgcgctgacgggcagcatcaccaggcggcgca<br>gaaggtgcatcgcgtgccgtccaacctgacgaccgcatccgccagctggaagccgatcttggcgttg<br>agctgtttatctgtagaaccagcgtttgcgttatctcccgcgggcataactcctcgcgtacagcaggc<br>agatcctgcctgtggtgatgaagcgcgatggtcgtcgcgggtgatgagccgaggggtattttgcct<br>cggcgcgctggaaagcaccgcccggctgcgcatcccgaacgctggcgcagtttaaccagcgcctat<br>ccgcgcatcagtttgcctttctaccgggctccgggacgatgattgatggcgtactggagggcacctta<br>agcggcctttgtagcgggcccgtgctgcacccggagctggagggcatgccggtctaccgggaag<br>agatgatgctagtacgcctcggggcacgcgaggttgacgcgccaagcaggttagcggcagcga<br>cgtttacgcatttcgcggaactgctcgtaccgtcgcacatctggaagctggttcatgaggacagacca<br>cgctggccgcatcagatgagatggagtctaccacggcatgctcgcctgctcattgcccggcgggca<br>tcgctgatgccgcgctcgtgctggagatgctcgggacatcatcaggtgaagcctggccgctgg<br>cggaaaactggcgtggcttacaacctggctggtggtggcggcgggcgatgacccggcagctgga<br>agctttatagcgtgctaaacgaacgtctcaaccagcgccttctcataa   |
| <i>ewb-9F12::Tn5</i> | atgccgcaaatcatcaggaagcgcgtgggagcgttttgcggagattacgtaatgcgcaaacgga<br>atgtattgtacgacagcaaagggagcagaacgctaggccagctatcactccgttatcccgcatttt<br>taccttcgacaaaccagacagcgtcgcctccctgcccgtatcgtctgcatcctctgatcgcacgttctc<br>cggggcatttacccttccggtagcggaaaacgatctggctttttacagtacacctcgggttcgacgg<br>gcttccgaagggcgtgatgggtgacctatggcaacctggtggccaactcgcgatgccattaccgcttttc<br>ggccatcacagcgaagccggggcagcagatctggctcccattttcatgatatggggctgattggcggg<br>ctactgcagcccgtttggcgcattcccctgctcgggtgatgtcggccatgatgtaataaaaaatcccctta<br>actggctcaaacatatttctgactatcaggcgcagcactccggcgccctaatttcgctacgatctgtgc<br>gtgcgcaagattggcagagagcaagttgaggcattagatcttctcgtgggatgtggcttttgcggcgc<br>agagccgattcggcccagcgtacagcagtttagcgaacactttgcgcccagggatttgcggcccg<br>gcgctcctgcctgctacggcatggcggaaccacgctcatcgtcaccgggatggagaaaggaca<br>agggctccgcttccgacgagggcggtagcgtgagctcgggcaggctcgcggataccgaggtgc<br>gatcgtcgtcccgatcgcacagccgcttctgatgtgagagcggggaatagggctcgtgctgctcc<br>gagcgttgcggcagatactgggacaatgacgcggccacacgcgaaacctccaggcgtctctgctg<br>gccatccgaccccgtggctgcgagcggcgatagggtttctccagtccggccatttgaactcaccgg<br>acgactcaagagctgctgattatcaacggtcagaacctaccgacggatattgaagagacgatcc  |

gccaggccgatcccgcgctggcgggaagcgacggttgctgtttgccagtgaaagacgagcgcccggtt  
gcgctgctgagctgatgacgcgccataaaaacgatctcgatatggcgacgctggcaccgtccgtgacc  
gcgcggtggcggagcggcacggcatcacgctggatgaactgctctgtcggcgaagggcaattc  
cccgcaccaccagcgggaaactacagcgcacccgcgaaagcgatgaccagcagggaaacct  
ggaagtagcctggcgcagctgccaggacgctcgaacctgtgaactcgggggaaacccacc  
cgctggtggcggctgatagccgggataatcagcagcgcgatgaacacgacgatcggcgaatcca  
gtgggacgagcgcttaccggcttggcatgagctctcgcaggcgggtggcggtgattggcgagctgaa  
cagcggctgggcccgcgagctctctcccgcgctgattatgactacccaccatcaatcggctggcggcc  
gcgctggggcaacccgctgcccggccggctcagctcagccgtcgggagagcgccattgctggg  
attggcatcggcgtggagctgcccggacatagcggcgtggaggcgtgtggtcgtcgtcgcagcagg  
ccacagcagcaccggcggagatcccggcgcaccgctggcgtacctcgtcccttgacggtttaaccgtaa  
aggcagtttctcgcagaggtcgacgcggttcgacgcaggctacttcggcatctctcccgtgaggccgtct  
atatgatccgcagcatcgtctgctgttagaaacggtcaacaggcgttaaccgatgcccggccttaaggc  
gtctccctgcgcggtagcgatacggcggcttctgtgggatcagcgcacgactacgcgctggcctgc  
ggcgataacgtctcggcctacagcggcttaggcaacgcgcacagatcgcggccaaccgaattcttat  
ctttatgattaaaaggccaagcgtcggcgcgacacggcctgttctctcgcgtggtggcgatagagg  
ggcaatgcagagcctgcgggcccggacggtgctcgtcggcattgccggaggcgtaactcggcgtgac  
gccacattgcaaaaagtctcaccgaagcccagatgctggccccgcagcgggtgtaaacctcaccctg  
acgcccgcgcggtatggctatgtctggtggcgaagggtggtggcgtggtgcttaagccgttcacaggc  
gctggcggatggcgatcgggttatgccacgctggtggcgagcgcggtgaatcaggcggcggcggc  
aacggcattaccgcgcaaatggccatcgcagcaggcggctacctcaggcggatggcggacgccc  
gggtggacagcgcagcattgactatacgaagcgcacggctacgggaaccgcgctggcgatctgatt  
gaatatcaggcgtggaagcgggttggcggaccggaaaaagaccgcacctgtccagggtgggttcgat  
caaaaccaacattggccacctgaggcggcggcggcgtgctggcggtgtaaacgtctctgatgc  
tgcacttccggcaatacgtacctcacctcaatttcagcagaaaaaccgcataattgcggcgattagccgt  
catgttgaggtagcggcgcgcagcctgcctcatggcatgccgatggcgaagcgcgctatgcggcgt  
aagcagcttggctcggcgggtaccaacggctatgtatgtgctcagcgcgccagcgggtgaaaaacg  
ccaggagcccgtcgcgcgcagcggcctgtctctggtcggttccatgataaggggctttaccctcag  
cgggaggcggcaaaaagggttatcgcagctccaggagagcgatattgccacctggtgctggcgtgt  
gaaacccgctacgacgcggcccgtatcgcggcgtggcgtatggcgcggatcgtcccagctggcg  
gaaagccttgcgcagctcaccgtctgaagggtgggtaaagcccagcccaggctggctctcccggg  
gcaggcaccagcaaatcggcatgggtgcccagctgtatcacctatcggcactatcgcaccagct  
ttgacgcgctggcgcagcactattcagcagcgtatcagattgatattacgcaggcgtgtttgccgtgac  
gacagctggcagcgtcgcgccagaacgtgcagctctcattattgctgtagctacgcgctgtctcagag  
cgtgatgcagttcggcccgcgtccggcgtgccgtaatggggcacagcctgggagagtagctgcggcgg  
ttatcgtggctatctcgtgagcagcggcgtggcaatggtcatcagcgcgctgttgatgtcagccc  
tgacgcaggaagggcgatggctgtctcagcggcgaagccgcagctccgtcagatgattccccct  
ggacgggcgacattgatattgccgattcaacacgcggacattgaccaccatcgcaggcagctcggcgc  
gcgattgacgcctgcctcaggccatctcaaaaggcggtcacgccagaaaaataaaactgccagc  
gcatttactctcgtatgatggatcctcggcgcctggcgcgagtggtggtcaacaacgtcacctt  
caccgcgggacgatcccgtttacagcaacctgaacggtagggcgtgcagccgaccgacgcggac  
tactggaccggcaaatcgcagcccgtgagttcctcaggggcgtgcaaacgctgctggcacagggt  
gagttcaccttatcgtatcgcagcggcgggttcgctgggcaaatgtgaccgcaactgaccgcccgtca  
ccgggtgctggcgcaggcgcagcggcgcagatgagtacaaatcactgctgacgctgctgggtacgctgt  
ggcagcaagggcacgacatcaactggagcgggctgtaccacgcgaccacgcgggaggcgtfaacc  
ctgcccgcctaccagttctgcccgaacggttactggctggcgggtgagacgccagcgcagaccatct  
gcaaaaggagcgtatgtcaaatcaacacctttagccgctgaaataaaagcgattattgccggtttct  
tgaggcggatcccgcgcttgacgactctcgtcggctcctggaaatggggcggactcgtggtgctg  
ctggatgcatcaataaccattaaagaccgcttggcgtagccatcccggcgcggcgtgttgaagagc  
tcaatacgtgagcgcggatcgatcgatgtggtggagcagcgcagccggcggctcgtcaccacc  
ccggaaaccgcccgtggcggcacagcctgtcgcggcaccgcagggtaccagcaggccgggtcct  
gatacggttcaggatctgattgccgcccagctggagctatgtcccagcagctaaattgttaacggcac  
ggcgcaggctctcccgatccagcccacccgcgacgcccggacgtatcgcgctcgcggcctgctg  
gccccagccgaccggtaaggccagcgcgcacaacagctggfttaaaaagagaccaaaaagggt  
ctccctcggcgtgagcgcgaccagcatctggcgcactcaccgaacggttgtcgataaaacggggc  
ggtcaaaacgcaatgccagcaataccgcggcgtcgcgggataaccgggctctgcccgttctgt



|                     |   |
|---------------------|---|
|                     | <p>cagatctgctttacctccgcttfcgcatatgtggatcaccggccgtacgatgatggcaaggcgattat<br/>cgccgggatggcggcagcgcacatcgcatctcagctatgttcaactggcgctgaaccgaaaatcat<br/>gggctggccctaacgccgtgatcgccgctgctgttggcttcgggatcgtgctggcggcgggtgga<br/>aaccggctggatgtaccgcccgtcgaaggccaggtacactactggtgggtggctgggaaatgttat<br/>cggctcagcatcctggcgtacttctggacgatctccccggcgtggccacgagctgggataaggt<br/>caacctgctgagcaccttcggccccctggcggcctgctggtcacctacgcccctgctggtgctttt<br/>actggtgtcgacaggagaaacgcttctccgcccgaagtgftaaacagaaaccaggagaatg<br/>ctgcatga</p>  |
| <i>ews-1H3::Tn5</i> | <p>atgacgagccgtaaacctgcccattctttactggtggatgacgatcccgggctgttaaagctgctgggat<br/>gctgctggtgagtgaaggctacagcgtgacccgcaaagcgggctggaggggctgaagatctc<br/>accgcgagaaaatcgatctggtgataagcgacctgcgatggacgaaatggatggcctgagctgtt<br/>cgcgggatccagaggcagcagccgggatgcccgtgatcattctgacggcgcacgggtgatcccg<br/>gatgcggtgcccgcagcagcagggggtcttcagcttctgaccaagccggtggacaaagacgcgt<br/>gtataaggctatcgacagcgcgtggaacatgcccggcgggggatgaagcgtggcgggagtc<br/>catcgtaccccgagccccattatgctgctctcctgaacaggccggatggtggcgcagctccgacgtc<br/>agcgtgctcatcaacggccagagcggaaaccgggaaagagatctggcccaggcagtcataacgcc<br/>agcccgcgagtaaaaatgctttatcgccattactgcccgcgcttcggaaacagcttctcgaatctg<br/>aactgttggctatgcccggcgcattcaccggcgcggtgagcagtcgggaaggcgtgtccaggcg<br/>gcggaaggcggcacgctgttctggacgagatggcgacatcccgcgcgctgagctgagctgagctg<br/>gcgctattgaggagcgaaggtcggcctgggacgcaaccgcatcgaatgaatgaatgctgca<br/>ttattccgcccaccggcagcttgcctgcaaaagtgtggcccgaacgagtttcgcaagatctacta<br/>ccgtctgaacgtggtgaatctgaagatccctgcgctggcggagcgcgcggaagacattccgctgctg<br/>gaatcatctctgcccaggcggccgatcgtcataaacctgttgccgctgttccaccgacgcgatga<br/>agcggctgatggccgaggctggccggtaacgtgcccagctggtgaacgtgattgagcagtgctg<br/>gcgctgacctctcaccggtaacagcagatgctgtagagcaggcgtggaaggagaaaaacagg<br/>cgtgcccagcttgcggaagcgcggaatcagttcagctgaactatctgcgcaagctattgcagatca<br/>ccaaaggcaacgtgaccacgcggcgcgatggccggacgcaaccgacccgagttctacaagctgc<br/>tgtcgcgccacgagctggaagcaaacgattttaagagtaa</p>   |
| <i>ewc-3H2::Tn5</i> | <p>atgaacaaaagaacattactcagtgcttattgctggcgcagtggtgacccgtttatggctcaggcaacc<br/>ctgctgcaggccagcagcgaaccttaccccttaaggccagcagatctgcagaagaaagcaggag<br/>ttaaccaactcccgtgatggctcgggtgaagtcaacctccgcacgctggacaacagcctggtgaa<br/>caaattgagcctgtaaatcgacaacccggaaaacgtaagcgcgtggaaggattatcaaggcca<br/>gagactgggattatcttcccactgctgcccggaaatatactacagcaacttctgaaagcgtgctg<br/>aaattcccggcactgtccagacctataccgatggtcgtaacagcagatgcatctgcccgaagctctg<br/>caacctgttcgpcacttcgpcaggaactggcggccacgagctcctggctccggaagccgagtg<br/>gcgtcaggcgtggttacgtgctgagatgggctggagcgaaggtcagaaggcggatataacggc<br/>gaatgaaccggatgtctggcaggggagacctggcggtaagacaagatggcgatttctg<br/>tagctatttggccggtgcaaacagctctcctataactacaactacggcccgttctgaaagcagatga<br/>cggcagctccgctactgctggacaaacctgagctggtggcggacacctggctgaacctgcttccg<br/>gatcttcttctgcctaccgacggccaaaaccaagcagctgaggtatcgacggcacatggca<br/>gccgaacgatcacgataaggcgaatggtctgtaccgggctcggagtgaccacgcagatcatcaac<br/>ggcggcgtggagtgtggcggcccagctgagatcgccagctcaaaaccgtatcaaaactacaag<br/>agttcgcaactacctgaaagtgcctgttccgttaacgaagtctgggctgcgcaacatgaagcagtt<br/>cgacgaaggcggctggtgcccgtgaagatctactgggaacaggactggggatggagcgcggatc<br/>cccgtcaggccagacctacttccagctggtgggtaccagacgccattcagcgcctttaaaggggt<br/>gactacaccaaagtgcgtaagcatttctcaatgtgaacgtggtgggtgaagcgggactccgacggc<br/>ggtgagcgcagcgaacccggcggcggaccctgtcgaacccaacggacgaaggcaacaccacggc<br/>gggcccagacgataaacccccgctccggacgataatacggcagcgggtaaacctgacccggct<br/>agcaaaaatcgggctccgggtgggtgagcgggtaaacgagtttctgaaacgctgctgctg<br/>accgacgaagacggtaacacctgactataacctggacggctccgaacggccagaccgtaagcggc<br/>gaagataaagcattattacctcaatgcgcccgaagtggcagcggcgcagcagctaccgatcaacct<br/>taccgtcagtgagggcagctgagcagcaccaccagctatacgtgaacgtacaggctaagcagacc<br/>aacggcggccagaccgggacttaccgacctggacctcaaaaacaaatggaaagcagggcagatc</p> |



|  |  |
|--|--|
|  | ccacggcacggtgctgctgtgtctggagatgatcattttatccgtcgctccaccgagccgcagcgcacc<br>atcaagtcgatgaagcgcacacacgagttacaccgtgggtaagccggggaagaaaagtaccta |
|--|--|

**Supplementary Table 7. Gene-specific primers used in quantitative real-time PCR analysis.**

| <b>Gene ID</b>              | <b>PCR primers</b>  |
|-----------------------------|---|
| ewpR                        | 5D7F: 5'- GGCATAACTTCCTGCGCTAC - 3'<br>5D7R: 5': CAGTACGCCATCAATCATCG - 3'        |
| ewpF1                       | PhzF1F: 5'- TTTTCTCACCGGGCGTTTC- 3'<br>PhzF1R: 5'- GTATGTGCGGAGCCGGTAA- 3'        |
| ewpF2                       | PhzF2F: 5'- AAATGGCGCAGCAGCATAA- 3'<br>PhzF2R: 5'- GTCGGTGCGCACGAAAA- 3'          |
| ewfR                        | D5F : 5'- GGGGACAGTAACGACGAAAC - 3'<br>D5R : 5'- CGGCAATCTGTCGATATGAA - 3'        |
| ewfD                        | FusE/MFPF: 5'- TGGCCGTGCGGGATAAT- 3'<br>FusE/MFPR: 5'- GGATCGATGGTGTAAGCACATC- 3' |
| ewfE                        | FusEF: 5'- CGTCGAGCCCACCTTTAGC- 3'<br>FusER: 5'- TCCGGCAATCTGTCGATATG- 3'         |
| ewgS                        | A8F 5: GGAGTCAAAACACGGAATTTACG - 3'<br>A8R 5: ATCTGATAAGCAGGGAAGATCTCTTT - 3'     |
| ewvC                        | B9F 5: TGTTTTATGCTTAAACTGGCGATT - 3'<br>B9R 5: CGAATGCGGTGGGATATCA - 3'           |
| 16SrDNA (housekeeping gene) | 799F: 5'- AACMGGATTAGATACCCKG- 3'<br>1492R: 5'- GGTTACCTTGTTACGACTT- 3'           |